

**Sedimentary record from the Canada Basin, Arctic Ocean: implications for late to middle Pleistocene glacial history**

Revised submission, by L. Dong et al.

The letter contains point-by-point replies to reviewer comments (replies are given in italics) and explanation of attendant changes, followed by a marked-up copy of the revised manuscript, including replies to side comments. For the ease of following the revision, replies to comments referring to specific lines are also given in side comments.

## Reviewer 1

### Comments

3 Materials and methods XRF data (counts) could be normalized using Al to discriminate between terrigenous and biogenic contributions of Ca and Mn.

*Agreed. Changes have been made accordingly.*

As Ca concentrations include both biogenic and terrigenous components, they do not need to be reported in this paper (or there should be a discussion on the presence of forams etc., also see comments below).

*Corresponding discussion has been added in section 5.2.*

Principal component analysis (PCA) is not clearly outlined and difficult to follow throughout the paper. More motivation could be provided in Ch. 3 Methods (lines 194-198) to explain why this analysis was undertaken (e.g. to distinguish between potential components in the sediment composition). Consequently, the selection of variables (sediment characteristics) should be explained. PCA is meant to restructure the dataset into several independent components. In this paper, mineral assemblages in bulk and clay fractions, contents of different grain-size fractions, and foraminiferal numbers were included in the PCA. If looking for potential forces/sedimentary environments, factor analysis would be a better choice over the PCA. Alternatively, the selection of variables to be included in the PCA could be reduced to mineral assemblages, for example. Then Fig. 7 and Fig. 8 could be combined to show the downcore PC scores. The procedure could be described stepwise (in Ch. 3 Methods or in Ch. 4.6 Results, PCA): 1) variables (sediment properties) are positively or negatively correlated with each of the identified PCs, 2) loadings of the variables on PCs 1-3 are used to group these variables.

*Parts of the MS related to PCA have been revised for clarity and more specifics. We have tested a Factor Analysis instead of the PCA, but the results were very similar, so we see no necessity to change the approach. We have also tested the analysis without total Ca and foraminifers, but again, the results did not differ significantly, so we are leaving the full suite of variables for a more comprehensive picture. Fig. 8 has been revised to show the downcore PC scores, as suggested by the reviewer.*

4.6 Principal component analysis Fig. 6, Table 3 and Fig. 8 should be revised. As stated by the authors, the PCs 1-3 contribute only to 54% of the total variance. Hence, interpretation of the PCA results is not straightforward (also see comments above). For example, clay mineral abundance is not grouping with the clay abundance (also see Ch. 5.2.4). In Fig. 6a, variables of groups 4 and 5 have very insignificant loadings on PC 1 and PC 2. In Fig. 6b, variables of groups 1,5,6 have very insignificant loadings on PC 2 and PC 3.

*PCA has been re-run to address the updates (normalized Ca, Mn). Text, figures, and tables related to the PCA have been revised to address the latest iteration and reviewer's comments. To improve the presentation, Fig. 6 (new Fig. 7) has been*

*moved to the Discussion with more explanation added.*

5.1 Stratigraphic framework What about absence of forams in B12 and B13? If this is due to dissolution, should you use abundance of forams as a variable with interglacial meaning in the PCA?

*We agree, the absence of foraminifers in these units, which is likely due to dissolution, can affect the performance of the foraminiferal variable in the PCA. However, foraminifers still show a consistent affinity to other interglacial proxies, so we prefer to leave them in a set of analysed variables for more comprehensive results. Test PCA runs without foraminifers did not produced considerably different results. Clarification has been added in section 5.2.*

5.2.2 North American provenance It is stated in line 477 that “dolomite is the main contributor of Ca in sediment cores from western Arctic Ocean”. However, it is not clear from the paper if this is true for core ARC4-BN05. There are several prominent peaks of forams observed, and calcite contents sometimes exceed those of dolomite (Table S1). Therefore, Ca elemental concentrations should not be attributed only to dolomite and used as an indicator of the NA provenance. This also applies to the comment about the PCA.

*We believe that a high correlation of the total Ca with dolomite (considerably higher than with calcite), and a consistent grouping of Ca and dolomite in the PCA results, confirms that dolomite is the main contributor to total Ca levels. Intervals with elevated calcite are low in total Ca. We note also that these intervals have mostly low foraminiferal numbers, so the biogenic origin of this calcite is not obvious.*

#### **Technical corrections**

4.4 Grain size Check the grain sizes of silt and clay fractions (lines 253, 257, and Fig. 4).

*Explanation to the choice of clay-silt cutoff size has been added.*

Table 1. Footnote should be added stating thereferences used.

*Done.*

Table 3. Footnote should be added explaining how the groups were identified (from Fig. 6).

*Table has been replaced by the PC loading score table.*

Table S4 (PCA loadings) can be included as one of the main tables for clarity.

*Done.*

Fig. 4. Stratigraphy could be shown, as this figure is discussed in Ch. 5.2.1.

*Showing the age model in Figure 4 would bring interpretation into the Results section, which should be avoided. We have added lithological indices or core depths in the discussion text to make it easier to follow.*

Fig. 7 should follow Ch. 5.1. Stratigraphic framework, as you start to discuss the proxy records vs. age in Ch. 5.2.

*Fig. 7 (new Fig. 6) is placed in section 5.1.*

## Reviewer 2

L 62-62: Existence of considerable ice masses on the onshore East Siberian margin is in serious reservations. A short article by Basilyan about glaciation on the New Siberian Islands is not convincing enough and raises many doubts, especially regarding the formation of interbedded ice, which the authors unreasonably considered to be relicts of glaciation (Basilyan et al., 2010). For example, geochemical studies of massive ground ices from the New Siberian Island showed their non-glacial origin (Ivanova, 2012, Earth's Cryosphere).

*We agree that the terrestrial evidence for glaciation on New Siberian Islands is insufficient for a conclusive interpretation, although we do not find a conclusive evidence against an ice sheet impact in the paper cited by the reviewer (Ivanova, 2012). We have added a clarification in the text; going into more detail would be nonessential in the overall context of the MS and distractive from its main line.*

L 212-214: Have you tried to identify the Clark units (except PW) in your Core? Why do you mentioned the PW layers, but nothing has been written about the other Clark units?

*We correlate our core with a nearby core PS72/392-5 that has been correlated in detail to Clark's reference core FL224 (Stein et al., 2010). To this end, it would be redundant to correlate BN05 additionally to FL224. We note that Clark's stratigraphy has been considerably revised and enhanced in more recent papers due to better sampling resolution and more comprehensive, up-to-date studies. "PW layers" is a legacy term introduced by Clark and commonly used for a distinct stratigraphic marker regardless of the overall Clark's stratigraphy (see Cronin et al., 2014, for more detail).*

L249-250: When characterizing the polymodal grain-size distribution of bottom sediments, it is meaningless to use the skewness and kurtosis (although these parameters can be technically calculated)! Using the skewness and kurtosis makes sense for unimodal curves only!

*Corrected.*

L 255-256: For a correct analysis of the modes in the plot of bottom sediments grainsize distribution, it is necessary to use a fixed distance between adjacent boundaries, which should correspond to a same module of geometric progression: ratio between neighboring fractions should have a constant value. Therefore, it is desirable to specify the number of fractions used during plotting the grain-size graphs. *We have used standard size bins used in the laser diffraction analysis. We believe that identifying principal modes in this data format provides sufficient information for the purpose of the study.*

L 285-289: I wonder why a maximum of dolomite in the B 11 sediment does not coincide with the Pw1 layer?

*There may be some offsets related to prevailing processes of sediment delivery or*

*variations in the exact provenance sources. As appears in core BN05, dolomite contents increases across the PW1 layer and reaches its peak right above it.*

L 340: Did you study the benthic foraminifera? If benthic forams were checked in sediments, then why you didn't put the information on their content? Probably, they are absent in section? Clarify please.

*Clarification added in section 4.1.*

L 353-355: Could you describe foraminifera in the layers "B14-16" in more details? What is their size (are they juvenile?), species? Is it possible to compare them with the foraminifera *Globigerina quinqueloba* from the Clark's unit "G" (Clark et al., 1990)? *Yes, the foraminiferal peak in B14-15 is predominated by *Turborotalida egelida*, previously referred to as *Globigerina quinqueloba* (e.g., in Clark et al. 1990). We have added clarification in section 5.1 with references to more up-to-date papers on this topic.*

L 405: Mode 2 "around 7-7.5 mkm is too coarse for suspension plumes: : :". It depends entirely on the water current velocities. Even at low currents speeds of 0.1 cm/s (or even less!) the particle of this size can be transported by currents in suspension without problems. You can check it on the "Hjulstrom curve".

*We agree that fine to medium silt can be carried by currents, but the enrichment in particles of this particular size, and the distinct difference from finer-grained intervals within glacial/deglacial units suggests a likelihood of a specific depositional process. The text has been adjusted for more clarity.*

L 540-542: The statement that the smectite, kaolinite and chlorite correspond to the East-Siberian Ice Sheet is questionable. The content of kaolinite and smectite in the sediments of the East Siberian Sea is not high (e.g. Stein, 2008; Wahsner et al., 1999). The high content of smectite and chlorite comes to the Chukchi Sea mainly through the Bering Strait and therefore occupy western part of the Chukchi Sea in a greater degree. In general, the content of chlorite is more or less close to the Siberian Arctic seas Can you confirm the link between clay minerals and fine sand statistically (by calculating the correlation coefficient)?

*We agree that stating the East-Siberian affinity of this group before discussing it was premature. The discussion to follow in section 5.2.4 explains our reasons for this linkage. The text has been adjusted accordingly.*

L 648-649: " : : , with Siberian sources predominating early and late glacial stages (MIS 12-14 and MIS 4-6, respectively): : :". Siberian sources really quite probable for MIS 4-6, however, are doubtful for the MIS 12, as it contains high amounts of dolomite (fig. 5).

*We agree, MIS12 has a mixed signature. The text has been corrected accordingly.*

L 1122-128 – FIG 1: In Figure 1, there is no difference between the Banks and

Victoria islands. However, Victoria Island is composed primarily with platformal dolomites, whereas Banks consists mainly of clastic rocks.

*We agree with the comment, but the schematic map used (Fagel et al., 2014) is inevitably generalized and does not provide a detailed resolution, which would be redundant at this scale. We note that based on the up-to-date glaciological reconstructions, major ice streams of the NW LIS sector flew via the main channels of the Canadian Archipelago rather than directly from the coasts facing the Arctic Ocean, which facilitated export of dolomitic rocks from the interior of the Archipelago.*

L 1158-1161 – Figure 5: For the convenience of sedimentary environments analysis, the distribution of the sand fraction should be added to the Figure 5.

*Done.*

---

1 **Sedimentary record from the Canada Basin, Arctic Ocean:**  
2 **implications for late to middle Pleistocene glacial history**

3 Linsen Dong<sup>a,b</sup>, Yanguang Liu<sup>a,b</sup>, Xuefa Shi<sup>a,b,\*</sup>, Leonid Polyak<sup>c</sup>, Yuanhui Huang<sup>a,b</sup>, Xisheng Fang<sup>a</sup>,  
4 Jianxing Liu<sup>a,b</sup>, Jianjun Zou<sup>a,b</sup>, Kunshan Wang<sup>a,b</sup>, Fuqiang Sun<sup>a</sup>, Xuchen Wang<sup>d</sup>

5 <sup>a</sup>Key Laboratory of Marine Sedimentology and Environmental Geology, First Institute of Oceanography, State  
6 Oceanic Administration, Qingdao, 266061, China

7 <sup>b</sup>Laboratory for Marine Geology, Qingdao National Laboratory for Marine Science and Technology, Qingdao, 26  
8 6061, China

9 <sup>c</sup>Byrd Polar and Climate Research Center, The Ohio State University, 43210, USA

10 <sup>d</sup>Key Laboratory of Marine Chemistry Theory and Technology, Ocean University of China, Qingdao, 266100,  
11 China

12

13 \*Corresponding author. Tel./fax: +86 532 88967491

14 E-mail address: [xfshi@fio.org.cn](mailto:xfshi@fio.org.cn) (X. Shi)

15

16 **Abstract:** Sediment core ARC4–BN05 collected from the Canada Basin, Arctic  
17 Ocean, covers the late to middle Quaternary (Marine Isotope Stages (MIS) 1-15, ca.  
18 0.5-0.6 Ma) as estimated by correlation to earlier proposed Arctic Ocean  
19 stratigraphies and AMS<sup>14</sup>C dating of the youngest sediments. Detailed examination of  
20 clay and bulk mineralogy along with grain size, content of Ca and Mn, and planktic  
21 foraminiferal numbers in core ARC4–BN05 provides important new information



---

22 about sedimentary environments and provenance. We use increased contents of coarse  
23 debris as an indicator of glacier collapse events at the margins of the western Arctic  
24 Ocean, and identify the provenance of these events from mineralogical composition.  
25 Notably, peaks of dolomite debris, including large dropstones, track the Laurentide  
26 Ice Sheet (LIS) discharge events to the Arctic Ocean. Major LIS inputs occurred  
27 during the stratigraphic intervals estimated as MIS 3, intra-MIS 5 and 7 events, MIS 8,  
28 and MIS 10. Inputs from the East Siberian Ice Sheet (ESIS) are inferred from peaks of  
29 smectite, kaolinite, and chlorite associated with coarse sediment. Major ESIS  
30 sedimentary events occurred in the intervals estimated as MIS 4, MIS 6 and MIS 12.  
31 Differences in LIS vs. ESIS inputs can be explained by ice-sheet configurations at  
32 different sea levels, sediment delivery mechanisms (iceberg rafting, suspension  
33 plumes, and debris flows), and surface circulation. A long-term change in the pattern  
34 of sediment inputs, with an apparent step change near the estimated MIS 7/8 boundary  
35 (ca. 0.25 Ma), presumably indicates an overall glacial expansion at the western Arctic  
36 margins, especially in North America.

37

38 **Keywords:** Sediment core, Pleistocene, western Arctic Ocean, clay minerals, bulk  
39 minerals, sediment provenance, Laurentide Ice Sheet, East Siberian Ice Sheet

40

## 41 **1. Introduction**

42 The advances and decays of continental ice sheets play a significant role in the  
43 alteration of global climatic system, such as changing atmospheric circulations,

---

44 creating large area albedo anomalies and regulating the global sea level fluctuations  
45 (Clark et al., 1990). Reconstruction of the history of ice sheets is therefore important  
46 not only for a better understanding of feedbacks of the future climate change and its  
47 impact on regional climates, but also for getting insights into the mechanisms of  
48 abrupt climate change.

49 Studies of Pleistocene glaciations around the Arctic Ocean dealt mostly with the  
50 late Quaternary history of the Eurasian Ice Sheet during Marine Isotope Stages (MIS)  
51 1–6(e.g., Svendsen et al.,2004;Larsen et al.,2006) or the Laurentide Ice Sheet (LIS)  
52 with a special attention to the Last Glacial Maximum (LGM)(e.g. Dyke et  
53 al.,2002;England et al., 2009).In addition to terrestrial data, studies of sediment cores  
54 from the Arctic Ocean are critical for comprehending the history of glacial advances  
55 and retreats (e.g., Polyak et al., 2004; 2009; Spielhagen et al., 2004; Stein et al.,2012;  
56 Kaparulina et al., 2015). However, the long-term history of circum-Arctic glaciations  
57 is still poorly understood, especially with respect to the western Arctic including the  
58 North America and East Siberia. A major impact of the North American ice sheets on  
59 circulation and depositional environments in the Arctic Ocean is indicated by various  
60 marine and terrestrial data (e.g., Phillips and Grantz, 2001; Stokes et al., 2005),  
61 [whereas](#), the East Siberian Ice Sheet (ESIS) remained largely hypothetical until  
62 recently. [While](#) terrestrial [data are limited and remain to be better investigated](#)  
63 [\(Grosswald, 1989; Basilyan et al., 2010; Ivanova, 2012\)](#), seafloor mapping data now  
64 provide [ample](#) evidence for the existence of considerable ice masses on the East  
65 Siberian margin (~~[Basilyan et al., 2010](#)~~; Niessen et al., 2013; Dove et al., [2014](#);

批注 [LP1]: R2: Existence of considerable ice masses on the onshore East Siberian margin is in serious reservations. A short article by Basilyan about glaciation on the New Siberian Islands is not convincing enough and raises many doubts, especially regarding the formation of interbedded ice, which the authors unreasonably considered to be relicts of glaciation (Basilyan et al., 2010). For example, geochemical studies of massive ground ices from the New Siberian Island showed their non-glacial origin (Ivanova, 2012, Earth's Cryosphere). See answer in the response letter.

---

66 | [Jakobsson et al., 2014, 2016](#)), but the timing and extent of these glaciations is  
67 | virtually unknown. Marine sedimentary records from the Arctic Ocean adjacent to the  
68 | East Siberian margin could add valuable information to this intriguing  
69 | paleoglaciological problem.

70 |       In this paper, we present a multiproxy study of glacial-interglacial changes  
71 | during the late to middle Pleistocene based on sediment core ARC4-BN05 from the  
72 | Canada Basin north of the Chukchi Plateau and east of the Mendeleev Ridge ([Fig. 1](#)).  
73 | This location can be affected by the two main Arctic Ocean circulation systems, the  
74 | Beaufort Gyre and the Transpolar Drift, which carry sea ice, icebergs, and sediment  
75 | discharge from the North America and Siberia, respectively. As this circulation along  
76 | with sedimentary environments and sources varied greatly during the Pleistocene  
77 | climate cycles, resulting variations in sediment delivery and deposition make for a  
78 | valuable paleoclimatic record for the western Arctic. Biogenic proxies (such as  
79 | foraminifers) have uneven and overall limited distribution in Arctic Ocean sediments,  
80 | while the terrigenous component provides a more consistent material for  
81 | paleoceanographic studies (e.g. Stein, 2008; Polyak et al., 2009). As sediments in the  
82 | Arctic Ocean are primarily transported by sea ice and/or icebergs during glacial  
83 | events, sediment composition yields important information not only on the  
84 | provenance and transport pathways, but also on the attendant glacial and  
85 | paleoclimatic history (e.g. Spielhagen et al., 1997; Vogt et al., 2001; Knies et al.,  
86 | 2001). By using clay and bulk mineralogy, along with grain size and the content of  
87 | major elements Ca and Mn, we reconstruct depositional environments and sediment

---

88 provenance to provide clues to the history of western Arctic ice sheets and their  
89 interaction with the Arctic Ocean.

90

## 91 **2. Regional background**

92 The Arctic Ocean is surrounded by land masses composed of an assortment of  
93 lithologies and situated in a variety of climatic, tectonic, and physiographic settings.

94 Figure 1 depicts a schematic geological map showing the main terrains and associated

95 lithologies (Fagel et al., 2014). The West Siberian Basin, ~~and~~ East Siberian platform

96 ~~and Verkhoyansk-Chukotka provinces~~ of the Eurasian continent are mainly composed

97 of terrigenous sediment (Fagel et al., 2014). The Siberian (Putorana) traps constitute

98 one of the largest flood basalts in the world (Sharma et al., 1992). The western

99 Okhotsk - Chukotsk volcanic belt contains acidic to intermediate rocks, whereas

100 intermediate to basic rocks are more characteristic of the eastern side (Viscosi-Shirley

101 et al., 2003). The Kara Plate and the Taymyr foldbelt, as well as the Ural and Novaya

102 Zemlya foldbelt are mainly composed of intrusive and metamorphic rocks (Fagel et

103 al., 2014).

104 The geology of outcropping terranes of Alaska mainly includes

105 Canadian-Alaskan Cordillera, Brooks Range, and part of the Northern-American

106 platform containing mostly intrusive, metamorphic, and some clastic rocks (Fagel et

107 al., 2014). The outcrops of the Canadian Arctic Archipelago are mainly composed of

108 carbonate and clastic rocks (Phillips and Grantz, 2001; Fagel et al., 2014), whereas

109 intrusive and clastic rocks are mostly characteristic for Greenland (Fagel et al., 2014).

---

110 Dissolved and suspended matter is transported to the Arctic Ocean by  
111 voluminous rivers, with the Lena and Mackenzie Rivers being the largest on the  
112 Siberian and North American side, respectively, both directly affecting the western  
113 Arctic Ocean. The transported material is further distributed across the Arctic Ocean  
114 in water and/or ice by currents. The two main surface, wind-driven circulation  
115 systems are the clockwise Beaufort Gyre (BG) in the western Arctic and the  
116 Transpolar Drift (TPD) that carries water and ice from the Siberian margin to the  
117 Norwegian-Greenland Sea (e.g., Rudels, 2009). The strength and trajectories of these  
118 current systems may vary depending on changes in atmospheric pressure fields known  
119 as the Arctic Oscillation (Rigor et al., 2002).

120 Sedimentation in the Arctic Ocean is strongly controlled by sea ice that acts as  
121 sediment carrier, but can also suppress sediment deposition under thick and persistent  
122 ice cover (Darby et al., 2006; Polyak et al., 2009). During glacial/deglacial events,  
123 multiple icebergs discharged into the Arctic Ocean from the termini of marine-based  
124 ice sheets and strongly affected sediment dispersal and deposition (e.g., Spielhagen et  
125 al., 2004; Polyak et al., 2009). Fine-grained sediments can also be transported by  
126 subsurface and deep-water currents, such as the Atlantic water (Winkler et al., 2002),  
127 but their role in the overall Arctic Ocean sedimentation is not well understood.

128 [\[Figure 1\]](#)

129

### 130 3. Materials and methods

131 Gravity core ARC4-BN05 (referred hereafter as BN05) was collected from the

批注 [LP2]: R1: Lena is not the only big river on the Siberian side. *This is correct, but we are just saying it is the largest one.*

---

132 Canada Basin in the vicinity of the Mendeleev Ridge(80°29.04'N, 161°27.90'W, 3156  
133 m water depth) (Figs. 1, 2) on the fourth Chinese National Arctic Research Expedition  
134 (CHINARE-IV) in 2009. The BN05 site was chosen in a close proximity to earlier  
135 investigated cores FL224 and PS72/392-5 ([Clark et al., 1980](#); Stein et al., 2010a) to  
136 enable robust correlation with the established stratigraphies. A total of 119 samples  
137 were taken at 2-cm intervals over the 238-cm BN05 length, and kept frozen until  
138 analyzed.

139 [\[Figure 2\]](#)

140 For age constraint within the radiocarbon range, Accelerator Mass  
141 Spectrometry<sup>14</sup>C dating was performed on 1000–1200 tests of planktic foraminifers  
142 *Neogloboquadrina pachyderma* sin. (>63 μ m) from core depths at 4-6, 8-10, 18-20  
143 and 22-24 cm, using the NOSAMS facilities at Woods Hole Oceanographic  
144 Institution.

145 For grain-size analysis, ~2-g sediment samples were successively treated with  
146 15 ml 15% H<sub>2</sub>O<sub>2</sub>, 5 ml 3mol/L HCl, and 20 ml 1mol/L Na<sub>2</sub>CO<sub>3</sub> for removing organic  
147 matter, biogenic carbonates, and biogenic silica, respectively. Grain size  
148 measurements in the range of 0.02 to 2000μm were performed on a Malvern  
149 Mastersize laser particle sizer (Mastersizer 2000) at the First Institute of  
150 Oceanography, SOA, China.

151 Coarse sediment >63 μm was sieved from ~10–15 g samples and counted under  
152 the microscope for foraminiferal and mineral grain numbers; [planktonic foraminiferal](#)  
153 [amounts were expressed as percent of the total grain numbers \(at least 300 grains per](#)

批注 [LP3]: R1: Do you use this  
anywhere?  
Explanation added.

154 sample counted).

155 Concentrations of major elements, such as Ca and Mn, were determined on point  
156 samples by ICP-OES (iCAP6300) at the First Institute of Oceanography, SOA, China,  
157 following the standard procedures. For a more detailed downcore distribution, relative  
158 Elemental abundances, given in peak area (counts per second, cps), were obtained at  
159 1 cm resolution using the Itrax XRF core scanner at the Polar Research Institute of  
160 China, setting at 20 s count times, 10 kV X-ray voltage and an X-ray current of 20  
161 mA. The obtained count values are used as estimates of relative concentrations. In  
162 addition, concentrations of major elements, such as Ca and Mn, were determined on  
163 point samples by ICP-OES (iCAP6300) at the First Institute of Oceanography, SOA,  
164 China, following the standard procedures. A good match of the ICP-OES and Itrax  
165 XRF data (Fig. 3) verifies the consistency of results. To account for the dilution  
166 effects on the background sedimentation, such as by coarse debris and biogenic  
167 processes, element contents were normalized to Al (e.g., März et al., 2011).

168 Color reflectance was measured using a hand-held Minolta CM-2002  
169 spectrophotometer at 1 cm intervals. Only the grayscale lightness index (L\*) is used in  
170 this paper.

171 A total of 60 2-cm-thick samples were collected at 4-cm interval for  
172 paleomagnetic measurements performed at the Paleomagnetism and Geochronology  
173 Laboratory of the Institute of Geology and Geophysics, Chinese Academy of Science.  
174 Magnetic susceptibility was measured using the KLY-4s Kappabridge instrument.  
175 Subsequently, stepwise alternating field (AF) demagnetization of natural remanent

批注 [LP4]: R1: As Mn has a redox sensitive nature and Ca is involved in biological processes, the XRF results are often normalized by the Al contents to discriminate between terrigenous and biogenic contributions.  
*Normalization applied per reviewer's suggestion.*

176 magnetization (NRM) was conducted using the 2-G Enterprises Model 760-R  
177 cryogenic magnetometer (2G760) installed in a magnetically shielded (<300 nT)  
178 space. AF demagnetization steps of 5-10 mT were used up to a maximum AF of 100  
179 mT.

180 For bulk sediment mineralogy ~5-g samples were dried, pulverized, passed  
181 through a ~~200 mesh~~ 63 μm sieve, and loaded into aluminum holders. Samples were  
182 X-rayed from 5 to 65° 2θ with Cu K-alpha radiation (40 kV, 100 mA) using a step  
183 size of 0.02° 2θ and a counting time of 2 s per step on a D/max-2500 diffractometer  
184 (XRD) equipped with a graphite monochromator with 1° slits in the laboratory of the  
185 First Institute of Oceanography, SOA, China. Prior to the analysis, instrument was  
186 blank corrected and all samples were measured under the same conditions. Peak areas  
187 were estimated from XRD traces using Jade6.0 software, and semi-quantitative  
188 estimates of bulk mineral percentages were calculated following Cook (1975). ~~The~~  
189 ~~windows (2θ), range of spacings (A) and intensity factors of minerals were~~  
190 ~~determined based on Cook (1975) are listed in~~ (Table 1).

191 Samples for clay minerals determination (~5g) were first treated with H<sub>2</sub>O<sub>2</sub> (10%)  
192 and HCl (1mol /L) to oxidize the organic matter and remove ~~the biogenic~~ carbonates,  
193 respectively. Clay fractions (<2 μm) were obtained by the Atterberg settling tubes  
194 method according to Stoke's Law. Each sample was transferred to two slides by wet  
195 smearing. Samples were then air-dried prior to XRD analysis. One sample slide was  
196 air dried at 60 °C for 2 h and analyzed. The second sample was solvated with ethylene  
197 glycol in an underpressured desiccator for at least 24 h at 60 °C. Every

批注 [LP5]: R1: indicate metric units  
Done

批注 [LP6]: R1: This sentence is  
redundant  
Deleted



198 ethylene-glycol solvated sample was measured twice: the first scanning was done  
199 from 3° to 30° 2θ with a step size of 0.02°, and the second scanning from 24° to 26°  
200 2θ with a 0.01° step. The latter was run as a slow scan to distinguish the 3.54/3.58 Å  
201 kaolinite/chlorite double peak. Clay minerals were also identified by X-ray diffraction  
202 (XRD) using a D/max-2500 diffractometer with CuKα radiation (40 kV and 100 mA)  
203 in the laboratory of the First Institute of Oceanography, SOA, China. Peak areas  
204 representing the clay mineral groups were estimated from glycolated XRD traces  
205 using the 17 Å smectite, 10 Å illite, and 7 Å chlorite plus kaolinite peaks. Chlorite (004)  
206 was identified at 3.54 Å and kaolinite (002) at 3.58 Å (Biscaye, 1964), respectively.  
207 Semi-quantitative estimates of clay mineral percentages were calculated by means of  
208 Biscaye's factors (1965).

209 To enhance the [identification of potential contributions from various sediment](#)  
210 [sources, and thus the](#) interpretation of downcore proxy [distributions](#), Principal  
211 Component Analysis (PCA) was performed in MATLAB [MathWorks, 2014]. [To](#)  
212 [account for proxies potentially indicative of sediment provenance and depositional](#)  
213 [processes and environments](#), PCA included all analyzed mineralogical proxies along  
214 with main grain-size groups (clay, silt, fine to medium sand (63-250 μm), and coarser  
215 grains), Ca and Mn concentrations, and foraminiferal numbers ([Table S1](#)). [A](#)  
216 [combined use of various sedimentological and geochemical data gives informative](#)  
217 [results in PCA application to paleoclimatic research, including studies of Arctic](#)  
218 [marine sediments \(Pelto, 2014; Simon et al., 2014\). The choice of variables for PCA](#)  
219 [performance was tested by Pearson correlation coefficients \(Table S3\).](#)

批注 [LP7]: R1: More detailed motivation/explanation needed, e.g. what would you like to explore by the means of the PCA - potential contributions from different sediment sources etc.  
*More explanation added.*

批注 [LP8]: R1: I suggest choosing a different combination of proxies or a different statistical method. For details see Specific comments.  
*See explanation in the response letter.*

220

## 221 4. Results

### 222 4.1 General stratigraphy

223 As common for sediment cores from the Arctic Ocean (e.g., Jakobsson et al.,  
224 2000; Polyak et al., 2004, 2009; Spielhagen et al., 2004; Stein et al., 2010a, b), core  
225 ARC4-BN05 displays distinct cycles in sediment color and composition expressed in  
226 interlamination of dark brownish and lighter-colored grayish muds (silty clays, clay  
227 silts and sandy silt), with coarser dropstones occurring in several layers. The color  
228 cyclicity is approximated by changes in sediment lightness that largely mirrors the  
229 content of Mn (Fig. 3), consistent with other studies from the Arctic Ocean (e.g.,  
230 Jakobsson et al., 2000; Polyak et al., 2004; [Löwemark et al., 2008](#); Adler et al., 2009).

231 We identify 18 distinctly brown units, from B1 to B18, characterized by elevated  
232 content of Mn (Fig. 3). Another prominent lithostratigraphic feature in the western  
233 Arctic Ocean, widely used for core correlation, is pink-white to whitish layers (PW)  
234 rich in detrital carbonates (e.g., Clark et al., 1980; Polyak et al., 2009; Stein et al.,  
235 2010a, b). We identify three major PW layers expressed both visually and in high Ca  
236 content (Fig. 3). [Lower Ca peaks occur throughout the record without being clearly](#)  
237 [expressed in the core macroscopic appearance.](#)

238 Foraminiferal abundances are generally high (mostly >50% of >63 $\mu$ m grains) in  
239 brown units, except for B11-B13 and below B17-B18, and are very low to absent in  
240 grey units. This pattern is consistent with foraminiferal stratigraphy reported in earlier

批注 [LP9]: R2: Have you tried to identify the Clark units (except PW) in your Core? Why do you mentioned the PW layers, but nothing has been written about the other Clark units?  
*Answered in the response letter.*

---

241 studies from the western Arctic Ocean (e.g., cores NP-26, HLY0503-JPC6 & 8,  
242 P1-92AR-P23 &39: Polyak et al., 2004, 2013; Adler et al., 2009; Cronin et al., 2013;  
243 Lazar and Polyak, 2016). [While only planktic foraminifers have been counted, data  
244 from correlative records indicate similar downcore variability in relative abundance of  
245 benthic foraminifers.](#)

246 [\[Figure 3\]](#)

247

#### 248 **4.2 AMS $^{14}\text{C}$ dating**

249 The measured AMS $^{14}\text{C}$  ages of core ARC4-BN05 were calibrated to calendar  
250 ages based on calibration using CALIB 7.10 (<http://calib.org/calib/calib.html>) (Table  
251 2). The reservoir corrections of 790 and 1400 years were applied to Holocene and  
252 glacial-age samples, respectively, according to Coulthard et al. (2010) and Hanslik et  
253 al. (2010). Same corrections have also been applied to  $^{14}\text{C}$  ages in core 03M03 from  
254 the Chukchi Abyssal Plain ([Fig. 2](#); Wang et al., 2013; [see Fig. 2 for location](#)).

255

#### 256 **4.3 Paleomagnetic stratigraphy**

257 While detailed paleomagnetic investigation is not an objective of this paper, we  
258 utilize the inclination data for an independent stratigraphic constraint in line with  
259 earlier studies (e.g., Jakobsson et al., 2000; Spielhagen et al., 2004; Polyak et al.,  
260 2009). Paleomagnetic inclination in core ARC4-BN05 shows mostly positive values

---

261 oscillating around  $+70^\circ$  in the upper part of the core, with a major polarity change  
262 occurring at  $\sim 120$  cm (Fig.3). A similar inclination drop has been identified in  
263 multiple sediment cores across the Arctic Ocean in the same stratigraphic position  
264 within estimated MIS7, although the nature of this change in paleomagnetic  
265 characteristics is not well understood (e.g., Jakobsson et al., 2000; Polyak et al., 2009;  
266 Xuan and Channell, 2010).

267 Other paleomagnetic parameters, such as magnetic susceptibility (MS), can  
268 provide additional correlation means (e.g., Sellén et al., 2010). Two prominent peaks  
269 in MS occur in the intervals between units B7/B8 and B10/ B11 (Fig. 3).

270

#### 271 4.4 Grain size and dropstones

272 Based on the results of grain-size analysis, sediment in core BN05 can be  
273 generally classified as sandy ~~mud, poorly to very~~ poorly sorted ~~mud, mostly~~  
274 ~~coarse skewed, and strongly leptokurtic (peaked)~~ (e.g., Blott and Pye,  
275 [2012](#)). ~~Generally Overall~~, silt and ~~clay~~ predominate grain-size composition (33-60%  
276 and 23-61%, respectively), but coarser particles also make a considerable contribution,  
277 with up to  $>30\%$  peak contents of sand ( $>63\mu\text{m}$ ) (Fig. 4a). We note that  $4\mu\text{m}$  was  
278 used as a cut-off size between clay and silt to account for overestimation of fine  
279 sediment diameters by laser diffraction, especially in the presence of platy particles  
280 (Beuselinck et al., 1998; Ramaswamy and Rao, 2006). Coarse size fractions, from  
281 coarse silt to various sand fractions (e.g.,  $>63$ ,  $>125$ , and  $>250\mu\text{m}$ ) mostly co-vary

批注 [LP10]: R2: When characterizing the polymodal grain-size distribution of bottom sediments, it is meaningless to use the skewness and kurtosis (although these parameters can be technically calculated)! Using the skewness and kurtosis makes sense for unimodal curves only!  
*Corrected.*

批注 [LP11]: R1: Indicate grain sizes here  
*Explanation added.*

---

282 downcore.

283 [\[Figure 4\]](#)

284 Grain size distribution is mostly polymodal with three distinct major modes  
285 centered at ~4, 7-7.5, and 85-90  $\mu\text{m}$ , plus a smaller but consistent mode at ~400-450  
286  $\mu\text{m}$  (Fig. 4b), which can be approximated by clay (<4  $\mu\text{m}$ ), silt, and sand size  
287 fractions, respectively. Mode 1 (4- $\mu\text{m}$ ) is overall most common in core BN05,  
288 occurring mostly in combination with the fine- and/or coarse-sand mode, but also  
289 forming very fine-grained intervals (e.g., at 37 cm, Fig. 4b). Mode 2 (7-7.5  $\mu\text{m}$ ) is  
290 common in the lower part of the core (below ~175 cm), where it mostly co-occurs  
291 with mode 1 and coarse-grain tail, and also in distinct grey units around 30-40 and  
292 90-100 cm in combination with the fine-sand mode 3 (e.g., 39 and 93 cm, Fig. 4b).

293 Several core intervals contain large rock fragments >5mm (dropstones). These  
294 rock fragments are mostly poorly rounded, subangular to angular in shape.  
295 Composition of sampled dropstones is illustrated in Fig. 4c. Most dropstones are  
296 represented by dolomite and low metamorphic quartz sandstone fragments of up to 5  
297 cm in diameter. Also found were individual dropstones composed of volcanic rock  
298 and shale, as well as a few greisen dropstones near the base of the core.

299

#### 300 4.5 Sediment mineralogy

301 The clay assemblage in samples from core ARC4-BN05 mainly consists of illite,  
302 chlorite, kaolinite and smectite (Fig.5).The illite group is overall the major constituent

批注 [LP12]: R1: Correct this or extend explanation, e.g. mixture of clay (<2  $\mu\text{m}$ ) and fine silt (2-63  $\mu\text{m}$ )  
*See explanation above*

批注 [LP13]: R2: For a correct analysis of the modes in the plot of bottom sediments grain size distribution, it is necessary to use a fixed distance between adjacent boundaries, which should correspond to a same module of geometric progression: ratio between neighboring fractions should have a constant value. Therefore, it is desirable to specify the number of fractions used during plotting the grain-size graphs.  
*Answered in the response letter.*

303 of the clay mineral fraction, ranging between 43% and 73%. Its downcore distribution  
304 pattern is opposite to that of the three other major clay-mineral groups - kaolinite,  
305 chlorite, and smectite (mostly present in very low contents), ~~which~~ These three groups  
306 ~~mostly largely~~ co-vary except for some lithostratigraphic intervals, such as PW layers.  
307 Elevated content of these clay minerals is characteristic for grayish sedimentary units.

308 [\[Figure 5\]](#)

309 The bulk mineral assemblage in core ARC4-BN05 mainly consists of quartz,  
310 K-feldspar, plagioclase, calcite, dolomite and pyroxene (Fig. 5). Quartz is generally  
311 the most abundant mineral ranging between 20% and 51% and typically peaking in  
312 grayish sediment units. K-feldspar, plagioclase and pyroxene (mainly augitic) mostly  
313 co-vary, with peaks in grey units in the upper part of the core, but more in brown units  
314 in the lower part starting from unit B10. Calcite has a high content in brown units of  
315 the upper part and much lower values below unit B9. Dolomite distribution shows  
316 distinct peaks reaching up to 53%, with the highest peaks occurring in or adjacent to  
317 the PW layers. Similar to other minerals, the pattern of dolomite distribution changes  
318 around unit B10, with maxima in thick grey units below and in thin interlayers within  
319 brown units above this stratigraphic level.

320

#### 321 4.6 Principal Component Analysis

322 The first ~~three-five~~ Principal Components identified by PCA with a Varimax  
323 rotation account for ~~19%, 18%, and 17%~~ of the total variance, with relatively evenly  
324 distributed communalities (Table 3). This ~~relatively low and evenly distributed~~

批注 [LP14]: R1: Very low contents.  
Consider the errors of the Biscaye  
method  
*Noted in the text*

批注 [LP15]: R2: I wonder why a  
maximum of dolomite in the B 11  
sediment does not coincide with the  
Pw1 layer?  
*See the response letter.*

325 ~~communality of the leading Pespattern presumably~~ reflects a complexity of  
326 multi-proxy ~~variables~~ characterizing sedimentary environments and provenance, and  
327 their strong variability occurring over multiple climatic cycles. To further test the  
328 PCA performance, we have also run a Factor Analysis with the Maximum Likelihood  
329 extraction, which produced similar factor loadings and variance explained, thus  
330 indicating the robustness of the results.

331 ~~Despite this variability, the PCs identify several robust variable groups as shown~~  
332 ~~in the PC loading score plots (Fig. 6). Most of the groupings are well reproduced in~~  
333 ~~PC1-2 and PC2-3 plots, with just a few differences, such as a configuration of coarse~~  
334 ~~grain size fractions (high PC1 loading score for silt vs. high PC3 score for fine sand).~~

## 336 5. Discussion

### 337 5.1 Stratigraphic framework

338 As no single existing chronostratigraphic method can comprehensively constrain  
339 the age of the Arctic Ocean Pleistocene sediments, the age model for core  
340 ARC4-BN05 was developed by correlating multiple proxies (such as paleomagnetic,  
341 foraminiferal, and lithological; see Figs. 3, 5), combined with <sup>14</sup>C ages in the youngest  
342 part of the record, to earlier established Arctic Ocean stratigraphies (e.g., Adler et al.,  
343 2009; Polyak et al., 2009, 2013; Stein et al., 2010a). Core PS72/392-5, raised very  
344 close to ARC4-BN05 and investigated in much detail (Stein et al., 2010a), was used to  
345 exemplify the correlation combined with <sup>14</sup>C ages in the youngest part of the

批注 [LP16]: R1 See comment to  
Line 194 (Methods)  
*More explanation added in Methods  
and Interpretation. See also the  
response letter.*

批注 [LP17]: R1: loadings for fine  
sand are less than 0.7, hence,  
insignificant  
*This part has been revised and  
more explanation provided (see Ch.  
5.2)*

346 record(e.g., Fig. 76).

347 [Figure 6]

348 The two  $^{14}\text{C}$  dates from the uppermost, 10-cm-thick brown sedimentary unit (B1)  
349 in core ARC4-BN05 clearly identify its Holocene age (Table 2; Fig. 3). Compilations  
350 of  $^{14}\text{C}$  ages from the surficial and downcore sediments in the western Arctic Ocean  
351 (Polyak et al., 2009; Xiao et al., 2014) indicate that the age of this unit extends from  
352 ~2-3 ka on top to ~10-11 ka at the bottom contact, although an accurate estimate is  
353 impeded by the uncertainties with the reservoir ages.

354 Two  $^{14}\text{C}$  dates of ca. 42-44 ka from the brown unit B2 (Table 2; Fig. 3)  
355 apparently fall into MIS 3, consistent with earlier stratigraphic results (e.g., Polyak et  
356 al., 2004, 2009; Adler et al., 2009; Stein et al., 2010a). These ages should be, however,  
357 considered as crude estimates as they are close to the  $^{14}\text{C}$  dating limit, and the age  
358 distribution in B2 has common inversions (e.g., Polyak et al., 2009). In cores with  
359 relatively elevated sedimentation rates this unit occurs as two distinct brown layers,  
360 indicated in some papers as B2a and B2b (e.g., Stein et al., 2010a, b; Wang et al.,  
361 2013). In core ARC4-BN05 this partitioning is less apparent due to low sedimentation  
362 rates, but the brownish sediment on top of the coarse detrital carbonate peak PW/W3,  
363 typically located between B2a and B2b, probably corresponds to B2a.

364 An abrupt increase in sediment age between closely spaced B1 and B2 in core  
365 ARC4-BN05 suggests a very condensed section or a hiatus between MIS1 and MIS3.  
366 This age distribution is common for the western Arctic Ocean, and has been attributed  
367 to very low to no sedimentation due to a very solid sea-ice cover or an ice shelf during

批注 [LP18]: R1: Make this Fig. 4.  
*We aim to avoid any interpretation  
in the Results section. To this end,  
the age model is illustrated along  
with the stratigraphy discussion.*



---

368 the Last Glacial Maximum in MIS2 (e.g. Polyak et al., 2009; Wang et al., 2013).

369 Below the range of  $^{14}\text{C}$  ages the age model is based entirely on proxy  
370 correlations with earlier developed Arctic Ocean stratigraphies (e.g., Fig. 76). This  
371 correlation is enabled by the cyclic nature of sediment lithology and attendant proxies,  
372 where brown and grayish units generally correspond to interglacial (or major  
373 interstadial) and glacial climatic intervals, respectively (e.g., Jakobsson et al., 2000;  
374 Polyak et al., 2004, 2009; Adler et al., 2009; Stein et al., 2010a, b). In addition,  
375 correlation tie points are provided by rare or unique events, such as prominent detrital  
376 carbonate peaks (PW/W), major paleomagnetic inclination swings, and changes in  
377 foraminiferal assemblages and abundance pattern.

378 According to this approach, we identify foraminiferal- and Mn-rich brown units  
379 B3-B7 and B8-B10 as warm substages of MIS 5 and 7, respectively (Figs. 3, 76). This  
380 age assignment is corroborated by the prominent detrital carbonate peaks PW2 and 1  
381 near the bottom of MIS5 and 7, respectively. Furthermore, the principal drop in  
382 paleomagnetic inclination in core ARC4-BN05 occurs in the lower part of MIS7,  
383 consistent with many cores from the Arctic Ocean (e.g., Jakobsson et al., 2000;  
384 Spielhagen et al., 2004; Adler et al., 2009; Polyak et al., 2009). Solidly grayish,  
385 foraminiferal- and Mn-poor unit separating brown units B2 and B3 is accordingly  
386 considered as related to glacial MIS4, and a similar unit between B7 and B8 – to  
387 MIS6. It is possible, however, that most of the fine-grained, greyish sediment was  
388 deposited during deglaciations following the actual glacial intervals, which may have  
389 been very compressed, similar to the LGM.

批注 [LP19]: R2: Did you study the benthic foraminifera? If benthic forams were checked in sediments, then why you didn't put the information on their content? Probably, they are absent in section? Clarify please.  
*Clarification added in section 4.1.*

390 Stratigraphy below MIS7 has been less investigated in prior studies, and [is more](#)  
391 [difficult to address due to often less distinct units and scarce to absent foraminifers,](#)  
392 [probably resulting from stronger dissolution \(e.g., ~~Best-Lazar~~ Lazar and Polyak, 2016\).](#)  
393 ~~¶~~Therefore the age model for the lower part of the core is more tentative. Nevertheless,  
394 a prominent oldest foraminiferal peak in units B14-B156 (Fig. 3) allows us to identify  
395 these units as MIS11 by comparison with other microfaunal records reported from the  
396 western Arctic Ocean (e.g., Cronin et al., 2013; Polyak et al., 2013). [While individual](#)  
397 [species have not been counted in ARC4-BN05, predominant planktic foraminifers in](#)  
398 [this peak are identifiable as \*Turborotalitaegelida\*, constituting a unique event in the](#)  
399 [Arctic stratigraphy \(see Cronin et al., 2013, 2014, for more detail\).](#)MIS13 and 15 have  
400 been tentatively assigned to Units B17 and B18 underlying a prominent grey interval  
401 attributed to MIS12. Overall, the record in core ARC4-BN05 is estimated to represent  
402 the last ca. 0.5-0.6 Ma, that is, most of the middle to late Quaternary with an average  
403 sedimentation rates of 4-5 mm/ka.

批注 [LP20]: B2: Could you describe foraminifera in the layers "B14-16" in more details? What is their size (are they juvenile?), species? Is it possible to compare them with the foraminifera *Globigerina quinqueloba* from the Clark's unit "G" (Clark et al., 1990)?  
*Clarification added; see also the response letter*

## 405 5.2 Depositional environments and sediment provenance

406 Distribution of various terrigenous components in Arctic sediment records  
407 carries information on sediment sources and depositional environments, and thus  
408 paleocirculation and changes in paleoclimatic conditions, such as connection to other  
409 oceans and build-up/disintegration of ice sheets (e.g., Bischof and Darby, 1997;  
410 Krylov et al., 2008; Polyak et al., 2009; Stein et al., 2010a, b; Yurco et al., 2010;

批注 [LP21]: R1: Not sure this is useful  
See discussion below (in 5.2.2)

411 Fagel et al., 2014). We utilize the data on clay and bulk minerals along with the grain  
412 size and total Ca and Mn distribution in core ARC4-BN05 to reconstruct changes in  
413 glacial conditions and circulation in the western Arctic Ocean during several glacial  
414 cycles extending to estimated ca. 0.5-0.6 Ma. In this work we capitalize on earlier  
415 studies on the distribution of bulk and/or clay minerals in surface and downcore  
416 Arctic Ocean sediments (e.g., Vogt, 1997; Stein, 2008; Krylov et al., 2014; Zou,  
417 2016), corroborated by more targeted provenance proxies, such as radiogenic isotopes  
418 ([Bazhenova, 2012](#); Fagel et al., 2014; [Bazhenova et al., 2017](#)), heavy minerals (Stein,  
419 2008; Kaparulina et al., 2015), composition of coarse debris (Bischof et al., 1996;  
420 Wang et al., 2013), and iron-oxide grains (e.g., Bischof and Darby, 1997; Darby et al.,  
421 2002).

422 To optimize the PCA results for clarifying relationships between various  
423 sedimentary proxies, we plotted the leading PC loading scores as biplots in the PC 1-2  
424 and PC 3-4 space (Fig. 7a). These plots help to identify several sedimentary variable  
425 groups with high loadings (>0.7 average) in at least one of the leading PCs. Group 1  
426 consists of various proxies characteristic of brown layers (primarily Mn, foraminifera,  
427 calcite, and clay, with an apparent affinity to chlorite). The opposing Group 2 includes  
428 most clay minerals except chlorite, with a proximity to sand and, to a lesser extent, silt  
429 size fractions. Bulk mineralogy proxies are largely represented by the opposing  
430 groups 3 and 4. Group 3 comprises feldspar, pyroxene, and more distant quartz and  
431 plagioclase. Group 4 builds around dolomite that has high loading scores in both PC 3  
432 and 4, along with bulk Ca, and shows affinity to Kfsp/Plag and Qz/Fsp indices. In

433 [addition to these groups revealed by the leading PC biplots, PC5 \(10% variance\)](#)  
434 [shows high scores for sand and coarser sediment, with silt as the main opposing](#)  
435 [variable.](#)

436 [To gain insight into stratigraphic changes in sedimentary environments and](#)  
437 [provenance, we plotted the distribution of the identified variable groups 1-4 using the](#)  
438 [combined downcore scores of PC 1-2 and PC 3-4 \(Fig. 7b\). A combination of the PC](#)  
439 [group composition and downcore variability provides useful guidance for interpreting](#)  
440 [major sedimentary controls and their stratigraphic evolution.](#)

441 [\[Figure 7\]](#)

442

### 443 **5.2.1 Grain size and depositional processes**

444 A variable, mostly multimodal distribution of grain size in core BN05 indicates  
445 multiple controls on sediment delivery and/or deposition. The prevailing mode 1 at ~4  
446  $\mu\text{m}$  ([Fig. 4b](#)), often in variable combinations with the fine-sand mode, is common for  
447 brown units, except for the oldest layers [B16-B18](#) (estimated MIS 13/15 and partly [11](#);  
448 [Fig. 6](#)). This [granulometric](#) pattern is similar to grain-size distribution with an average  
449 mode at ~3.4  $\mu\text{m}$  reported for Holocene sediments across the Arctic Ocean (Darby et  
450 al., 2009). Furthermore, sediment in core BN05 with the same mode also makes up  
451 the most fine-grained intervals in glacial/deglacial units, such as MIS 4 and [6](#) ([at](#)  
452 [~30-40 and 100-110 cm](#); [Fig. 4b](#)). We infer that mode 1 represents some combination  
453 of deposition from sea ice and from suspension that could result from winnowing of

批注 [LP22]: R1: If you want to discuss the age distribution, show this in Fig. 4  
*We avoid showing the age interpretation before it has been discussed*

批注 [LP23]: R1: Ages are not shown in Fig. 4, hence, it is difficult to follow this discussion  
*Lithostratigraphic indices have been inserted for guidance*

---

454 fines from the basin margins and ridges during interglacials, as well as overflow  
455 plumes discharged by retreating glaciers during glacial/deglacial intervals. An  
456 occurrence of apparently similar grain-size pattern in interglacial and fine-grained  
457 glacial/deglacial intervals might indicate a convergence of glacial erosion processes  
458 with those related to sea-ice formation and transportation. A similar grain-size  
459 interpretation has been earlier proposed for sediment from the Canada Basin with the  
460 principal mode at  $\sim 2 \mu\text{m}$  (Clark et al., 1980). This apparent discrepancy may be  
461 related to the methodological offset between grain size determined by the pipette  
462 method vs. laser diffraction, where the latter produces larger diameters for fine  
463 sediment, especially in the presence of platy particles (Beuselinck et al., 1998;  
464 Ramaswamy and Rao, 2006).

465 Mode 2 centered at 7-7.5  $\mu\text{m}$  is more stratigraphically restricted. Its combination  
466 with the fine-sand mode (e.g., Fig. 4b) is characteristic for coarser grained portions of  
467 MIS 4, 6, and 12 ([~ 25-30, 40-45, 90-95, and 205-215 cm](#)), which also have a specific  
468 mineralogical composition ([PC loadingsedimentary variable](#) group [42](#); Fig. [67](#); Table  
469 [3](#)). This stratigraphic pattern suggests that the formation of this sediment was related  
470 to glacial/deglacial processes; however, the prevailing grain size mode around 7-7.5  
471  $\mu\text{m}$  is [distinctly coarser than in deglacial intervals characterized by mode 1 and likely](#)  
472 [deposited from](#) suspension [plumes, which suggests a different sedimentation regime.](#)  
473 [While being](#) too fine-grained for massive deposition from icebergs, fine to medium  
474 silts [are](#) susceptible to intermediate currents [and](#) are [thus](#) common for turbiditic  
475 deposits, including glaciogenic environments (e.g., Wang and Hesse, 1996; Hesse and

批注 [LP24]: B2: Mode 2 “around 7-7.5 mkm is too coarse for suspension plumes: : :”. It depends entirely on the water current velocities. Even at low currents speeds of 0.1 cm/s (or even less!) the particle of this size can be transported by currents in suspension without problems. You can check it on the “Hjulstrom curve”  
*Explanation added; see also the response letter.*

---

476 Khodabaksh, 2016). We propose that mode 2 sediment type is related to glacial  
477 underflows that formed debris lobes on glaciated margins grading into turbidites in  
478 the adjacent basins, along with iceberg-rafted debris. Multiple debris lobes have been  
479 mapped on the Chukchi and East-Siberian slopes in association with glacial  
480 diamictos on the margin (Jakobsson et al., 2008; Niessen et al., 2013; Dove et al.,  
481 2014). Close to the margins glaciaturbidites can form deposits of several meters thick  
482 (Polyak et al., 2007), but thin out towards the inner parts of the basins, such as the  
483 BN05 site. In particular, deposits similar to fine-grained turbidites, attributed to  
484 MIS4/lower MIS3, have been recovered from the Northwind and Chukchi basins  
485 affected by glacial inputs from the Chukchi and East Siberian margins,  
486 respectively (Polyak et al., 2007; Matthiessen et al., 2010; Wang et al., 2013). In the  
487 Chukchi Basin this unit, correlative to a much thinner MIS4 interval in core BN05, is  
488 characterized by a high content of fine silt with a peaky downcore distribution (Wang  
489 et al., 2010, 2013).

490 Additionally, modes 1 and 2 make up a bimodal distribution in the lowermost  
491 part of the core – mostly in estimated MIS 13/15 and near the bottom of MIS11. The  
492 predominant stratigraphic position in brown units makes unlikely the glacial origin  
493 of this sediment. We hypothesize that this grain-size pattern reflects a combination of  
494 “normal” interglacial environments with winnowed silts deposited by downwelling of  
495 shelf waters enriched in dense brines. Although no observational evidence exists for  
496 such waters penetrating deeper than the halocline (~200 m) under modern Arctic  
497 conditions, periods of stronger cascading in the past have been inferred from sediment

---

498 distribution on the slopes (Darby et al., 2009) and some sedimentary proxies, such as  
499 radiogenic isotopes (Haley and Polyak, 2013; Jang et al., 2013). The bimodal  
500 distribution of fine sediment in the lower part of the record is accompanied in most  
501 samples by a small but consistent coarse-sand mode (400-450  $\mu\text{m}$ ), likely indicating  
502 the presence of iceberg rafting.

503 Coarse sediment, up to dropstones of several cm large, is a consistent feature in  
504 core BN05. In the apparent absence of strong current control on sedimentation, except  
505 for some shelf areas, and a pervasive presence of floating ice, coarse sediment in the  
506 Arctic Ocean is typically attributed to ice rafting, including sea ice and icebergs (e.g.,  
507 Stein, 2008; Polyak et al., 2010, and references therein). Sedimentological studies in  
508 areas of sea-ice formation or melting and in ice itself indicate that sediment carried by  
509 sea ice in the Arctic Ocean is predominated by silt and clay, while coarser fractions  
510 are of minor importance (Clark and Hanson, 1983; Nürnberg et al., 1994; Hebbeln,  
511 2000; Darby, 2003; Dethleff, 2005; Darby et al., 2009). Some studies suggest a higher  
512 content of sand in ice formed at the sea floor (anchor ice) (Darby et al., 2011), but the  
513 contribution of this source yet needs to be evaluated. Furthermore, the role of sea ice  
514 on sedimentation in the Arctic Ocean is not clear for glacial intervals, when most of  
515 the sediment entrainment areas were exposed or covered by ice sheets. In contrast, in  
516 iceberg-rafted sediment, deposited mostly in glacial/deglacial environments, the  
517 content of large size fractions, from sand to boulders, is typically high, in excess of  
518 10-20% (Clark and Hanson, 1983; Dowdeswell et al., 1994; Andrews, 2000). Thus,  
519 elevated content of coarse sediment can be regarded as a good indicator of intense

---

520 iceberg rafting. Such events are not probable during full interglacials, exemplified by  
521 modern conditions, but most likely occurred at times of instability and disintegration  
522 of ice sheets that extended to the Arctic Ocean in the past (e.g., Spielhagen et al., 2004;  
523 Stokes et al., 2005; Polyak et al., 2009).

524 In core BN05, coarse fractions (from coarse silt to sand) measured at different  
525 sizes show very similar distribution patterns (Fig. 4a), indicating the same  
526 predominant delivery mechanism, that is, iceberg rafting. This pattern is reflected in a  
527 good correlation of fine to medium sand (63-250  $\mu\text{m}$ ) with coarser,  $>250\mu\text{m}$  fractions,  
528 that defines one of the [Principal Components \(PC 5: Fig. 6, Table 3\)](#). Increased  
529 coarse-grain content mostly characterizes grayish units, especially near gray-to-brown  
530 sediment transitions, and the PW layers, but also occurs in brown units in the upper  
531 part of the record. The latter peaks enriched in detrital carbonates (high dolomite and  
532 total Ca) represent interstadial or incomplete interglacial conditions, such as MIS3,  
533 MIS5a, and parts of MIS7 ([Fig. 6](#)).

534 A common occurrence (separate or combined) of two coarse grain modes,  
535 around 85-90 and 400-450 $\mu\text{m}$ , may indicate different sources for iceberg-rafted  
536 material or different thresholds for glacial disintegration of various rock types. While  
537 a more thorough interpretation requires further research, we note that grain-size mode  
538 1 may co-occur with both fine- and coarse-sand modes, mode 2 – only with the  
539 fine-sand mode, and bimodal 1/2 sediment type – only with the coarse-sand one.

540



---

541 **5.2.2 North American provenance**

542 One of the most robust sedimentary variable groups is distinctly characterized by  
543 high loadings of dolomite along with total Ca content (Group ~~24~~: Fig. ~~67a~~, Table 3).

544 ~~Dolomite is known as a robust indicator of the North American provenance in the~~  
545 ~~western Arctic, especially in relation to glacial inputs (e.g., Vogt, 1997; Zou, 2016).~~

546 Dolomite has been proposed as the main contributor of Ca in sediment cores from the  
547 western Arctic Ocean, with an especially high content in multiple coarse-grain peaks

548 of detrital carbonates (Bischof et al., 1996; Phillips and Grantz, 2001; Polyak et al.,  
549 2009; Stein et al., 2010a, b). High correlation ( $r=0.81$ ) and consistent PC grouping of

550 dolomite and total Ca (Fig. 7a) corroborates their affinity in ARC4-BN05, although  
551 calcite can also contribute to Ca content ( $r=0.58$ ), especially in interglacial intervals

552 with high foraminiferal numbers. We note that total Ca may be a redundant proxy in  
553 the presence of dolomite and calcite data; however, it is convenient for a comparison

554 with a growing number of cores analyzed for elemental composition using XRF  
555 scanners (e.g., Löwemark et al., 2008; Polyak et al., 2009).

556 The main western Arctic source for dolomite is the extensive, carbonate-rich  
557 Paleozoic terrane in the northern Canada (North American Platform; Fig. 1; Okulitch,

558 1991; Harrison et al., 2008). During the Pleistocene this terrane has been repeatedly  
559 impacted by the LIS with a subsequent transport of eroded material into the western

560 Arctic Ocean (e.g., Stokes et al., 2005; England et al., 2009). The distribution of  
561 dolomite in Arctic sediment cores is thus a robust indicator of the North American

562 provenance and can be used for reconstructing the history of the LIS sedimentary

批注 [LP25]: R1: proxy for?  
See revised explanation below

批注 [LP26]: R1: It is not clear from the paper if the statement “dolomite is the main contributor of Ca in sediment cores from western Arctic Ocean” is true for core ARC4-BN05. There are several prominent peaks of forams observed, and calcite contents sometimes exceed those of dolomite (Table S1). Therefore, Ca elemental concentrations should not be attributed only to dolomite and used as an indicator of the NA provenance. This also applies to the comment about the PCA.  
See revised explanation and the response letter.

---

563 inputs.

564 Consistent with other cores from the western Arctic Ocean, overall high [dolomite](#)  
565 content in core ARC4-BN05 has major peaks corresponding to visually identifiable  
566 PW/W layers enriched in coarse debris (Fig.5). As has been suggested in earlier  
567 studies (e.g., Stokes et al., 2005; Polyak et al., 2009), we infer that the dolomite peaks  
568 are related to pulses of massive iceberg discharge from the LIS during the periods of  
569 its destabilization and disintegration. Furthermore, radiogenic isotope studies  
570 demonstrate that fine sediment in the dolomitic peaks also has North American  
571 provenance ([Bazhenova, 2012](#); Fagel et al., 2014; [Bazhenova et al., 2017](#)). These  
572 results indicate that dolomite may have been transported not only by icebergs, but also  
573 in meltwater plumes coming during deglaciations from the Canadian Archipelago or  
574 the Mackenzie River.

575 As noted above, a change in the stratigraphic pattern of dolomite distribution  
576 occurs around unit B10 estimated to correspond to the lower part of MIS 7 (Fig.6). In  
577 older sediments dolomite maxima co-occur with glacial (predominantly gray)  
578 intervals, whereas, in the younger stratigraphy dolomite peaks in brown sediment or  
579 grayish interlayers within brown units (MIS 3, 5, and 7), presumably corresponding to  
580 transitional paleoclimatic environments, such as interstadials or stadials within  
581 complex interglacial stages.

582 [Other potential mineral indicators](#) related to the North American provenance are  
583 quartz/feldspar [and K-feldspar/plagioclase ratios as exemplified by the BN-05 PCA](#)  
584 [results \(Group 4: Fig. 7a\), consistent with earlier studies \(e.g., Vogt, 1997; Zou, 2016;](#)

585 [Kobayashi et al., 2016](#)). [High Qz/Fsp ratio has been related](#) to a considerable presence  
586 of sedimentary rocks enriched in quartz, but not feldspar, in the Canadian Arctic in  
587 comparison with the Siberian margin (Vogt, 1997; Zou, 2016; Kobayashi et al., 2016).  
588 In core ARC4-BN05 the distribution of this index is generally similar to dolomite ([Fig.](#)  
589 [5](#)), except for some [coarse-grain peaks intervals](#), notably low Qz/Fsp values in PW1  
590 and [3](#) ([Fig. 6](#)) [resulting in an overall lower correlation \(r=0.46\)](#). [This pattern may be](#)  
591 [related to grain size variance or might reflect provenance differences. Low plagioclase](#)  
592 [content has also been identified for intervals with high detrital inputs from the](#)  
593 [Canadian Arctic \(Vogt, 1997; Zou, 2016\). Especially high Kfsp/Plag values](#)  
594 [accompany dolomitic peaks in the older glacial intervals corresponding to MIS 12 and](#)  
595 [10 \(Figs. 5, 6\)](#).

596

### 597 5.2.3 Siberian provenance

598 Mineral proxies potentially linked to Siberian provenance make two distinct  
599 groups, as reflected in the PCA results (Groups [32](#) and [-43](#); [Fig. 67a](#), Table 3). Group  
600 3 comprises primarily pyroxene, feldspar, and plagioclase, and strongly anticorrelates  
601 with the North-American proxies, [such as Qz/Fsp and primarily](#) dolomite. The  
602 downcore distribution pattern of this group changes from the affinity to interglacials  
603 in the lower part of the record to peaks in glacial/deglacial intervals related to MIS 4  
604 and 6 ([Fig. 7b](#)). The major source for pyroxene in the Arctic Ocean is the Siberian  
605 trap basaltic province that drains to the Kara Sea and western Laptev Sea (Fig. 1;

批注 [LP27]: R1: This ratio can be sensitive to the grain size of sediments. In core ARC4-BN05, Qu/Fsp does not correlate with the dolomite contents. If you want to use Qu/Fsp as an indicator of the N.A. provenance, you should discuss these issues  
*Agreed. Clarification added.*

---

606 Washner et al., 1999; Schoster et al., 2000; Krylov et al., 2008). On the other hand,  
607 basaltic rocks related to the Okhotsk-Chukotka province (Fig. 1) may have also  
608 provided a significant source of pyroxenes, as exemplified in surface sediments by a  
609 relative pyroxene enrichment in the Chukchi Basin on the background of overall low  
610 values in the western Arctic Ocean (Dong et al., 2014). Distributions of feldspar and  
611 plagioclase at the Siberian margin show elevated contents occurring both in the  
612 western Laptev Sea and the East Siberian Sea (Zou, 2016).

613       Based on a considerable affinity of the pyroxene-feldspar group to brown units  
614 and a lack of correlation with coarse sediment fractions, we infer that it is primarily  
615 related to sea-ice transport during interglacial/deglacial intervals, with sources  
616 potentially including the East Siberian margin and more westerly areas. The  
617 difference in both the sources and delivery processes from the LIS proxies may  
618 explain an especially strong opposition of these groups. Multiple studies suggest that  
619 sea ice from the Kara and Laptev seas may transport sediments to the Canada Basin  
620 under favorable atmospheric conditions, such as the positive phase of the Arctic  
621 Oscillation (Behrends, 1999; Darby et al., 2003; Darby et al., 2004; Yurco et al., 2010;  
622 Darby et al., 2012), although it remains to be investigated, to what extent this  
623 circulation pattern could have provided a significant sediment source for the western  
624 Arctic Ocean in the Pleistocene.

625

---

626 **5.2.4 East-Siberian Ice Sheet**

627 ~~Another leading sedimentary variable group with a potentially Siberian~~  
628 ~~provenance~~(Group 4: Fig.6, Table 3) comprises primarily clay minerals smectite,  
629 kaolinite, and chlorite, and shows affinity to coarse sediment, especially consistently  
630 to fine sand (63-250  $\mu\text{m}$ ) (Group 2: Fig.7a, Table 3). This composition is especially  
631 characteristic for intervals estimated as MIS 4, 6, and 12. The association of clay  
632 minerals with coarse sediment (correlation reaching as high as  $r=0.65$  for kaolinite) is  
633 unusual and suggests that they may have been derived by glacial erosion of source  
634 hard rocks. This linkage has been elaborated for kaolinite distribution in the Barents  
635 Sea and central Arctic Ocean (Junttila, 2007; Vogt and Knies, 2009; Krylov et al.,  
636 2014). While kaolinite sources, such as Meso-Cenozoic paleosols and shales, are  
637 mostly known in the western Arctic from northern Alaska and Canada (Naidu et al.,  
638 1971; Darby, 1975; Dalrymple and Maass, 1987), kaolinite weathering crusts have  
639 been also described from the East Siberian margin (Slobodin et al, 1990; Kim and  
640 Slobodin, 1991). Smectite, which is typically related to chemical weathering of basic  
641 rocks has been mostly associated in Arctic sediments with delivery from Siberian trap  
642 basalts (Fig. 1) as reflected in the surface sediments, suspended particulate material,  
643 and sea-ice samples from the Kara Sea and western Laptev Sea (Stein et al.,1994;  
644 Wahsner et al.,1999; Schoster et al., 2000;Dethleff et al., 2000). Peaks of smectite  
645 related to that source are especially characteristic for deglacial intervals in sediment  
646 cores from the eastern Arctic Ocean (Vogt and Knies, 2008). However, considerable  
647 sources of smectite also exist further east along the Siberian margin due to basaltic

批注 [LP28]: R1: Clay mineral assemblages were investigated in the < 2  $\mu\text{m}$  fraction  
*We did not mean that clay minerals were measured in coarse fractions (the word "related" was misleading). The point is, their distribution is similar to that of coarse sediment. The proposed explanation is discussed below.*

批注 [LP29]: R2: The statement that the smectite, kaolinite and chlorite correspond to the East-Siberian Ice Sheet is questionable. The content of kaolinite and smectite in the sediments of the East Siberian Sea is not high (e.g. Stein, 2008; Wahsner et al., 1999). The high content of smectite and chlorite comes to the Chukchi Sea mainly through the Bering Strait and therefore occupy western part of the Chukchi Sea in a greater degree. In general, the content of chlorite is more or less close to the Siberian Arctic seas  
Can you confirm the link between clay minerals and fine sand statistically (by calculating the correlation coefficient)?  
*We agree that stating the East-Siberian affinity of this group before discussing was premature. The discussion to follow explains our reasons for this linkage.*

---

648 outcrops related to the Okhotsk-Chukotka volcanic province(Fig. 1), resulting in high  
649 content of smectite in surface sediments of the East Siberian and Chukchi seas (Naidu  
650 et al., 1982; Viscosi-Shirley et al., 2003; Nwaodua et al., 2014).Chlorite is also  
651 common insurface sediments and suspended particulate material at the East Siberian  
652 margin(Dethleff et al., 2000; Viscosi-Shirley et al., 2003). Modern and Holocene  
653 sediments on the Chukchi shelf are especially enriched in chlorite due to advection  
654 from the North Pacific at high sea-level stands (Kalinenko, 2001; Ortiz et al., 2009;  
655 Nwaodua et al., 2014; Kobayashi et al., 2016), however this mechanism is only  
656 applicable to interglacial periods.

657 We infer that sediment with a concerted enrichment in smectite, kaolinite, and  
658 chlorite clay minerals associated with coarse fractions was transported to the Canada  
659 Basin primarily in relation to the existence of large ice sheets in northern East Siberia  
660 during glacial periods. Radiogenic isotope signature in upper Quaternary records from  
661 the Mendeleev Ridge also indicates that the Okhotsk-Chukotka volcanic rocks  
662 provided one of the principal end members, especially during MIS 4 and 6  
663 ([Bazhenova, 2012](#); Fagel et al., 2014; [Bazhenova et al., 2017](#)). This sediment had to  
664 be transported into the Arctic Ocean directly from the East-Siberian/Chukchi margin  
665 as the alternative pathway via the Bering Sea only operated at high interglacial sea  
666 levels, when the Bering Strait was open for throughflow (e.g., Keigwin et al., 2006;  
667 Ortiz et al., 2009).Considering an affinity of the kaolinite-smectite-chlorite group with  
668 sediments coarser than clays, corresponding to grain-size modes 2 and 3, their  
669 distribution across the basin was likely related to iceberg rafting and glacial

---

670 underflows, as discussed above in section 5.2.1. A relatively fast and direct delivery  
671 mechanism by debris flows and ensuing turbidites may explain a good preservation of  
672 fragile clay minerals, normally not resistant to physical erosion.

673       Some early paleoglaciological studies proposed the existence of a thick  
674 Pleistocene ice sheet centered over the East Siberian shelf (Hughes et al., 1977;  
675 Grosswald and Hughes, 2002). The inference of former ice sheets/shelves in this  
676 region is now corroborated by multibeam bathymetry and sub-bottom data revealing  
677 multiple glacial features on the top and slopes of the Chukchi and East Siberian  
678 margin (Polyak et al., 2001, 2007; Jakobsson et al., 2008, 2014, 2016; Niessen et al.,  
679 2013; Dove et al., 2014). ESIS has also been reproduced by numerical paleoclimatic  
680 modeling for a large Pleistocene glaciation exemplified by MIS6 (Colleoni et al.,  
681 2016). Sedimentary proxies indicative of the Okhotsk-Chukotka provenance in cores  
682 from the Canada Basin [may](#) provide an additional tool for reconstructing the ESIS  
683 history.

684

### 685 **5.2.5 Interglacial signature**

686       Data points from brown units make up a distinct [sedimentary variable](#) ~~PC loading~~  
687 group with Mn, foraminiferal numbers, [calcite](#), and fine sediment as lead variables  
688 (Group 1: Fig. [67a](#); Table 3). This composition is consistent with the modern-type  
689 Arctic Ocean environments characterized by predominant controls of sediment  
690 deposition by sea ice, considerable biological activity in summer, and high sea levels.

---

691 The latter is important for providing supply of Mn from the surrounding shelves  
692 (März et al., 2011; Löwemark et al., 2014). The same condition may also control  
693 biological production, and thus foraminiferal numbers, via export of nutrients from  
694 the marginal seas (e.g., Xiao et al., 2014), although interaction of this factor with  
695 sea-ice conditions yet needs to be clarified. [We note that the absence \(dissolution\) of](#)  
696 [foraminiferal tests in brown units corresponding to MIS9 and below MIS11 likely](#)  
697 [weakens their relationship to other interglacial proxies. Nevertheless, the](#)  
698 [foraminiferal variable shows a consistent proximity to Mn, clay, and calcite in the](#)  
699 [PCA results \(Fig. 7a\).](#)

700 The mineral having the closest distribution to [the main constituents of PC Group](#)  
701 [is illite](#), consistent with a predominant occurrence in brown, interglacial/major  
702 interstadial units ~~,are illite and calcite~~(Figs. 5, [67a](#)). Illite is atypical high-latitude clay  
703 mineral, mainly supplied by physical weathering of metasedimentary and plutonic  
704 rocks (Chamley, 1989; Junttila, 2007). High illite concentrations in surficial Arctic  
705 Ocean sediments have been found in many areas including the Alaska margin and  
706 adjacent Canada basin (Dong et al., 2014; Kobayashi et al., 2016), East Siberian Sea  
707 and the adjacent part of the Laptev Sea (Wahsner et al., 1999; Kalinenko, 2001;  
708 Viscosi- Shirley et al., 2003; Dethleff, 2005; Zou., 2016),and northern Greenland and  
709 Svalbard regions (Stein et al., 1994). In core ARC4-BN05 illite has consistently high  
710 values in generally fine-grained brown units (Fig. 5), although peak values may not  
711 exactly coincide with those of Mn or foraminiferal numbers. In addition, illite shows a  
712 prominent peak in a very fine-grained interval at ~35 cm within glacial/deglacial



---

713 sediment of estimated MIS4. This distribution is consistent with the pattern in both  
714 surface sediments and sediment cores, where illite is characteristic for fine-grained  
715 sediment indicative of transportation by sea ice or in the water column (Krylov, 2014).  
716 As shown by sediment-core studies, these mechanisms can provide high illite levels  
717 under both interglacial (this study) and glacial/deglacial environments (Knies and  
718 Vogt, 2003; Yurco et al., 2010). The latter is probably associated with deposition of  
719 fine sediment from glacial overflows, as exemplified by the fine-grained part of MIS  
720 4 deglaciation.

721 High contents of calcite in core ARC4-BN05 mostly co-occur with high numbers  
722 of foraminifers (Fig. ~~3 and 67a~~; Table 3), indicating that calcite in these sediments is  
723 to a large extent biogenic, consistent with earlier results from the study area (Stein et  
724 al., 2010a). Nevertheless, in the lower part of the record, where calcareous fossils are  
725 mostly not preserved, calcite shows a considerable affinity to dolomite, which  
726 corroborates a mixed, biogenic and detrital nature of calcite in Arctic Ocean  
727 sediments (e.g., Vogt, 1997).

728

### 729 **5.3 Evolution of sedimentary environments**

730 The stratigraphically changing pattern of sediment delivery and deposition,  
731 including cyclic glacial-interglacial fluctuations and longer-term changes, indicates  
732 complex interactions of climatic and oceanographic factors controlling depositional  
733 environments in both glacial and interglacial intervals. ~~To gain more insight into these~~

changes, we plotted the distribution of PC scores grouped by individual glacial and interglacial stages, along with the PC loading interpretation (Fig. 8).

A long-term trend in interglacial environments is indicated by a shift from (+) predominantly Siberian to more North American provenance, especially strong in MIS 5 and 1, and (2) from negative to increasingly positive-high scores of interglacial proxies (Group 1), with a threshold around the bottom of MIS 7 (Fig. 8a7b). Glacial environments show an apparently more complex provenance change, with Siberian sources predominating early and late glacial stages (MIS 12-14 and MIS 4 and 6, and Laurentide provenance controlling MIS 8 and 10 (Fig. 87b). Earlier glaciations, exemplified by a prominent MIS 12 unit, have a mixed signature of high smectite and dolomite contents, likely reflecting a combination of East-Siberian and LIS inputs. In addition, interglacial-type signature (Group 1) characterizes some intervals in MIS 4 and 6 as well as intermittent (stadial) intra-MIS 3, 5, and 7 events. We note that MIS 2 is not represented in this data due to its very compressed nature.

### 5.3.1 Glacial environments

The identified changes in sedimentary environments and provenance can be explained by several types of controls, including configuration of ice sheets against sea level and climatic conditions, sediment delivery mechanisms, and circulation. Ice sheet sites and geometry at specific time intervals dictate the timing and location of major sediment discharge events into the Arctic Ocean. Transportation mechanisms,

批注 [LP30]: R2: “with Siberian sources predominating early and late glacial stages (MIS 12-14 and MIS 4-6, respectively)” Siberian sources really quite probable for MIS 4-6, however, are doubtful for the MIS 12, as it contains high amounts of dolomite (fig. 5)  
*We agree, MIS12 has a mixed signature, and correct the text accordingly.*

---

755 such as by icebergs, debris flows, or suspension plumes, further control sediment  
756 delivery to specific sites. Finally, oceanic circulation affects the distribution of  
757 sediment across the oceanic basins. This may include surface circulation driving  
758 seaice, icebergs, and surface plumes, deep circulation affecting turbidite/contourite  
759 pathways, and downwelling of sediment-laden dense waters.

760 We infer that sedimentary variations observed in core BN05 and correlative  
761 records from the western Arctic Ocean can be explained by the evolution of  
762 surrounding ice sheets and associated changes in oceanic conditions, such as  
763 circulation, sea ice, and biota. It has been known from early studies (e.g., Clark et al.,  
764 1980; Winter et al., 1997) that glacial, notably LIS impact on the western Arctic  
765 Ocean has been steadily increasing over the time span covered by sediment cores  
766 from this region. A recent investigation utilizing a more up-to-date stratigraphic  
767 paradigm estimated the timing of a step increase in LIS inputs as ca. 0.8 Ma (Polyak  
768 et al., 2013), consistent with the onset of major glaciations in the Northern  
769 Hemisphere (Head and Gibbard, 2015). Core BN05 provides a record of sediment  
770 deposition in the Canada Basin, and thus glacial inputs into the western Arctic Ocean  
771 during most of the time interval to follow.

772 Considering the overall gradual growth of Pleistocene Arctic ice sheets, we infer  
773 that the shift from Siberian to North American sources between MIS 12 and 10 was  
774 primarily related to the expansion of the LIS, especially the northwestern Keewatin  
775 sector that discharges into the western Arctic Ocean. However, its further growth may  
776 have had an opposite effect due to a more massive ice sheet that required warmer

---

777 climatic conditions and/or higher sea levels to destabilize it. Based on data for the last  
778 glacial cycle, the Keewatin sector of the LIS rested mostly on relatively elevated  
779 terrane of the Canadian Archipelago and adjacent mainland, fringed by a narrow  
780 continental shelf and dissected by numerous channels providing conduits for ice  
781 streams and evacuation of icebergs at rising sea levels (Stokes et al., 2005, 2009;  
782 England et al., 2009; Margold et al., 2015). The latter events are illustrated in BN05  
783 data by intra-MIS 5 stadials with a consistent LIS signature ([Group 4: Fig. 87b](#)).  
784 Especially high LIS scores characterize PW layers 2 and 3 attributed to MIS 5d and  
785 late MIS 3, respectively. A similar, LIS-dominated pattern likely represents the last  
786 deglaciation as indicated by a number of provenance studies (e.g., Stokes et al., 2005;  
787 [Bazhenova, 2012](#); Jang et al., 2013; [Bazhenova et al., 2017](#)).

788 In comparison to the LIS, a presumably much smaller ESIS, formed on a broad  
789 and overall flat East-Siberian/Chukchi margin (Niessen et al., 2013; Dove et al., 2014;  
790 Colleoni et al., 2016), had to be responsive to sea-level changes even at low levels. It  
791 may be possible that the ESIS also increased in size by MIS 6, known as a time of a  
792 dramatic increase of glacial inputs from the Barents-Kara Ice Sheet into the eastern  
793 Arctic Ocean (e.g., O'Regan et al., 2008). A synchronous MIS 6 expansion of both  
794 North American and Siberian ice sheets and related ice shelves might explain the  
795 deep-keel glacial erosion of the Lomonosov Ridge at modern water depths exceeding  
796 1000 m (Jakobsson et al., 2016, and references therein).

797 A concurrent interpretation can be proposed with a focus on sediment  
798 transportation processes as deposits of some glacial intervals, notably MIS 12 and

---

799 parts of MIS 4 and 6, are associated with grain size mode 2 potentially indicating  
800 glacial debris flow/turbidite emplacement. Large debris flows entering the Chukchi  
801 Basin and continuing as turbidites into Canada Basin, as exemplified by subbottom  
802 sonar profiles (Niessen et al., 2013; Dove et al., 2014), may have overprinted  
803 deposition from icebergs. We note that deposits of MIS 4 and 6 also contain intervals,  
804 where Siberian provenance is combined with interglacial positive scores ([Group 1:](#)  
805 [Fig. 87b](#)) due to their fine-grained composition along with high illite content. These  
806 sediments likely represent deposition from suspension plumes, potentially marking  
807 especially strong deglacial meltwater discharge. A prominent fine grained, finely  
808 laminated interval within MIS4 deglaciation (possibly extending into MIS3) has been  
809 reported from multiple cores across the Chukchi Basin – Mendeleev Ridge area  
810 (Adler et al., 2009; Matthiessen et al., 2010; ~~Bazhenova, 2012~~; Wang et al., 2013;  
811 [Bazhenova et al., 2017](#)).

812 Under modern conditions the BN05 site is mostly controlled by the Beaufort  
813 Gyre current circulation system, although can also be affected by the Transpolar Drift  
814 during strong shifts in the Arctic Oscillation (Rigor et al., 2002). This setting  
815 probably applies to the Holocene and comparable interglacial conditions (Darby and  
816 Bischof, 2004). Some authors suggested that during glacial periods the surface  
817 circulation that controls pathways of iceberg and sea-ice drift may have been  
818 considerably different from the modern pattern, with both North American and  
819 Siberian sources shortcutting the Arctic Ocean towards the Fram Strait (Bischof and  
820 Darby, 1997; Stärz et al., 2012). These changes would have potentially affected the

---

821 study area, possibly making it more exposed to the Siberian provenance than under  
822 present conditions. However, the existing reconstructions based on very limited  
823 records with only crude stratigraphic controls, need to be elaborated by spatially and  
824 stratigraphically more representative data constraining past circulation changes. In  
825 particular, glacial maxima may be elusive, especially in the western Arctic Ocean, due  
826 to extremely low sedimentation rates or a hiatus, as exemplified by the Last Glacial  
827 Maximum (Polyak et al., 2009; Poirier et al., 2012).

828 An overall integration of potential controls on sediment deposition in the study  
829 area during major identified types of glacial environments are illustrated in Fig. 98.  
830 More studies are needed to discriminate between different controls, including proxy  
831 records providing higher resolution for target intervals as well as modeling  
832 experiments to test spatial and stratigraphic variability in such factors as iceberg and  
833 meltwater discharge and their ensuing distribution pathways.

834 [\[Figure 8\]](#)

835

### 836 5.3.2 Interglacial environments

837 The long-term trend in interglacial environments reflected in a shift from  
838 negative to increasingly positive scores of interglacial proxies ([Group 1: Fig. 7b](#)), with  
839 a threshold around the bottom of MIS 7 ([Fig. 8a](#)), can be partially explained by the  
840 absence of calcareous foraminifers in the lower part of the record. However, even  
841 MIS 11 that has abundant foraminifers ~~is in the~~ [has low](#) interglacial ~~negative~~

---

842 | [domainscores](#), suggesting more controls. One possibility is that this trend was related  
843 | to the evolution of circum-Arctic ice sheets that would have inevitably incurred  
844 | changes in oceanic conditions, such as circulation and sea ice. An expansion of  
845 | perennial sea ice in the western Arctic Ocean near the MIS 7 bottom has been  
846 | proposed based on foraminiferal assemblages (Polyak et al., 2013; Lazar and Polyak,  
847 | 2016). This step change has been tentatively attributed to the LIS growth that may  
848 | have affected sea-ice conditions via increased albedo and/or higher meltwater inputs.  
849 | This inference is consistent with a [coeval](#) change from [mostly](#) Siberian ([Group 3](#)) to  
850 | North American ([Group 4](#)) provenance during interglacials in BN05 (Fig. [8a7b](#)). In  
851 | addition to a more lingering LIS during interstadials/interglacials, this shift in  
852 | provenance could be related to a strengthening of the Beaufort Gyre as more sea ice  
853 | filled the western Arctic Ocean.

854 | More limited sea-ice cover in the older part of the middle Pleistocene could have  
855 | also enhanced the production of dense brines at the Siberian margin, resulting in a  
856 | deeper convection and cascading of shelf sediments to the deep basin. This scenario  
857 | would explain an unusual grain-size composition of sediments in the older  
858 | interglacials combining mode 2, indicative of winnowed silt, with a typical  
859 | interglacial fine-grained mode 1.

860

## 861 | **6. Summary and conclusions**

862 | Sediment core ARC4–BN05 was collected from the Canada Basin in the vicinity

---

863 of the Chukchi Plateau and the Mendeleev Ridge, Arctic Ocean, on the fourth Chinese  
864 National Arctic Research Expedition (CHINARE-IV). Based on correlation to earlier  
865 proposed Arctic Ocean stratigraphies (e.g., Adler et al., 2009; Stein et al., 2010a;  
866 Polyak et al., 2013) and AMS<sup>14</sup>C dating of the youngest sediments, the BN05 record  
867 covers the late to middle Quaternary (MIS 1-15, ca. 0.5-0.6 Ma). The core was  
868 investigated for multiple sedimentary proxies including clay and bulk mineralogy,  
869 grain size, paleomagnetism, elemental content, and planktonic foraminiferal numbers  
870 with an average estimated age resolution of 4-5 ka per sample. This study, facilitated  
871 by Principal Component Analysis of major paleoceanographic variables, provides  
872 important new information about sedimentary environments and provenance in the  
873 western Arctic Ocean on glacial time scales. The results enhance our knowledge on  
874 the history of Arctic glaciations and interglacial conditions.

875       Glacially derived sediment can be discriminated between the North American  
876 and Siberian provenance by their mineralogical and textural signature. In particular,  
877 peaks of dolomite debris, including large dropstones, track the Laurentide Ice Sheet  
878 (LIS) discharge events, while the East Siberian Ice Sheet (ESIS) inputs are inferred  
879 from combined peaks of smectite, kaolinite, and chlorite associated with coarse  
880 sediment. Siberian provenance is also identified from high content of pyroxene,  
881 feldspar, and plagioclase, unrelated to coarse sediment. This sedimentary signature is  
882 interpreted to indicate sea-ice transport from the Siberian margin during  
883 interglacial/deglacial intervals. Full interglacial environments are characterized by  
884 overall fine grain size, high content of Mn (and resulting dark brown sediment color),



---

885 and elevated contents of calcite and chlorite. Foraminiferal tests are abundant in  
886 interglacial units in the upper part of the record (MIS 1-7) and estimated MIS 11, but  
887 have very low numbers in other interglacials older than MIS 7, apparently due to  
888 dissolution.

889 In addition to glacial-interglacial cyclicity, the investigated record indicates  
890 variable impacts of LIS vs. ESIS on sediment inputs at different glacial events, along  
891 with a long-term change in middle to late Quaternary sedimentary environments.  
892 Based on the age model employed, major LIS inputs to the study area occurred during  
893 MIS 3, intra-MIS 5 and 7 events, MIS 8, and MIS 10, while ESIS signature is  
894 characteristic for MIS 4, MIS 6 and MIS 12. These differences may be related to  
895 ice-sheet configurations at different sea levels, sediment delivery mechanisms  
896 (iceberg rafting, suspension plumes, and debris flows), and surface circulation. A  
897 long-term shift in the pattern of sediment inputs shows an apparent step change near  
898 the estimated MIS 7/8 boundary (ca. 0.25 Ma), consistent with more sea-ice growth in  
899 the Arctic Ocean inferred from benthic foraminiferal assemblages (Lazar and Polyak,  
900 2016). This development of Arctic Ocean paleoenvironments possibly indicates an  
901 overall glacial expansion at the western Arctic margins, especially in North America.  
902 Such expansion may have affected not only glacial, but also interglacial conditions via  
903 increased albedo and/or higher meltwater inputs, as well as a strengthening of the  
904 Beaufort Gyre circulation as more sea ice filled the western Arctic Ocean.

905

## 906 **Acknowledgements**

---

907 We are grateful to the team of the 4<sup>th</sup> Chinese Arctic Research Expedition for their  
908 assistance with sample collection. Special thanks to Dr. Shijuan Yan for help with  
909 sampling and to Dr. Quanshu Yan for help in paper editing. This work was jointly  
910 supported by the Research Foundation of the First Institute of Oceanography, State  
911 Oceanic Administration of China (No. 2013G07, 2014G30), the Chinese Polar  
912 Environment Comprehensive Investigation & Assessment Programmes (No.  
913 CHINARE 2017-03-02), and the National Natural Science Foundation of China  
914 (No.41306205, 41676053, 40176136). [L.Polyak's participation was supported by the](#)  
915 [US National Science Foundation award ARC-1304755. Comments from two](#)  
916 [anonymous reviewers helped improving the manuscript.](#)  
917 \_\_\_\_\_

---

## References

- 918
- 919 [1] Adler, R. E., Polyak, L., Ortiz, J. D., Kaufman, D. S., Channell, J. E.T., Xuan, C., Grotoli, A. G., Sellén,  
920 E., Crawford, K. A.: Sediment record from the western Arctic Ocean with an improved Late Quaternary  
921 age resolution: HOTRAX core HLY0503-8JPC, Mendeleev Ridge, **Global and Planetary Change**,  
922 68,18-29,2009.
- 923 [2] Andrews, J. T.: Icebergs and iceberg rafted detritus (IRD) in the North Atlantic: Facts and assumptions,  
924 **Oceanography**, 13(3), 100–108, 2000.
- 925 [3] Basilyan, A.E., Nikol'skiy, P.A., Maksimov, F.E., Kuznetsov, V.Y.: Age of Cover Glaciation of the New  
926 Siberian Islands Based on <sup>230</sup>Th/U-dating of Mollusk Shells, **Structure and Development of the**  
927 **Lithosphere**, Paulsen, Moscow, pp. 506-514, 2010.
- 928 [4] [Bazhenova, E.: Reconstruction of late Quaternary sedimentary environments at the southern Mendeleev-](#)  
929 [Ridge \(Arctic Ocean\), PhD Thesis, University of Bremen, Bremen, 83 p, 2012.](#) [Bazhenova, E., Fagel, N.,](#)  
930 [Stein, R.: North American origin of “pink–white” layers at the Mendeleev Ridge \(Arctic Ocean\): New](#)  
931 [insights from lead and neodymium isotope composition of detrital sediment component, \*\*Marine\*\*](#)  
932 [Geology](#), 386, 44–55, 2017.
- 933 [5] Behrends, M.: Reconstruction of sea-ice drift and terrigenous sediment supply in the Late Quaternary:  
934 heavy-mineral associations in sediments of the Laptev-Sea continental margin and the central Arctic  
935 Ocean, **Reports on Polar Research**, 310, 1-167, 1999.
- 936 [6] Beuselinck, L., Govers, G., Poesen, J., Degraer, G., Froyen, L.: Grain-size analysis by laser  
937 diffractometry: comparison with the sieve-pipette method, **Catena**, 32, 193–208, 1998.
- 938 [7] Bischof, J.F. and Darby, D.A.: Mid-to Late Pleistocene ice drift in the Western Arctic Ocean: evidence  
939 for a different circulation in the past, **Science**, 277, 74–78, 1997.
- 940 [8] Bischof, J.F., Clark, D.L., Vincent, J.S.: Origin of ice-rafted debris: Pleistocene paleoceanography in the  
941 western Arctic Ocean, **Paleoceanography**, 11, 743–756, 1996.
- 942 [9] Biscaye, P.F.: Distinction between kaolinite and chlorite in recent sediments by X-ray diffraction,  
943 **American Mineralogist**, 49, 1281–1289, 1964.
- 944 [10] Biscaye, P.F.: Mineralogy and sedimentation of recent deep-sea clay in the Atlantic Ocean and adjacent  
945 seas and oceans, **The Geological Society America Bulletin**, 76, 803–832, 1965.
- 946 [11] [Blott, S.J. and Pye, K.: Particle size scales and classification of sediment types based on particle size](#)

---

947 [distributions: review and recommended procedures, \*Sedimentology\*, 59, 2071–2096, 2012.](#)

948 [\[11\]\[12\]](#) Chamley, H.: Clay Sedimentology, **Springer**, Berlin. 623 pp, 1989.

949 [\[12\]\[13\]](#) Clark, D. L., Whitman, R. R., Morgan, K. A., Mackey, S. D.: Stratigraphy and glacialmarine  
950 sediments of the Amerasian Basin, central Arctic Ocean, **Geological Society of America**, Special Paper,  
951 181, 57, 1980.

952 [\[13\]\[14\]](#) Clark, D. and Hanson, A.: Central Arctic Ocean sediment texture: a key to ice transport  
953 mechanisms. In: **Molnia, B.F. (Ed.), Glacial-Marine Sedimentation, Plenum Press**, New York, pp.  
954 301–330, 1983.

955 [\[14\]\[15\]](#) Clark, D. L., Chern, L. A., Hogler, J. A., Mennicke, C. M., Atkins, E. D.: Late Neogene climate  
956 evolution of the central Arctic Ocean, **Marine Geology**, 93, 69–94, 1990.

957 [\[15\]\[16\]](#) Colleoni, F., Kirchner, N., Niessen, F., Quiquet, A., Liakka, J.: An East Siberian ice shelf during  
958 the Late Pleistocene glaciations: Numerical reconstructions, **Quaternary Science Reviews**, 147, 148–163,  
959 2016.

960 [\[16\]\[17\]](#) Cook, H. E., Johnson, P.D., Matti, J.C., Zemmels, I.: Methods of sample preparation and X- ray  
961 diffraction data analysis, X-ray mineralogy laboratory, In: **Kaneps AG**, ed. Init Repts, DSDP XXVIII,  
962 999 -1007, <http://www.deepseadrilling.Org/28/ volume/dsdp28- appendix-IV. Pdf>, 1975.

963 [\[17\]\[18\]](#) Coulthard, R.D., Furze, M.F.A., Pienkowski, A.J., Nixon, F.C., England, J.H.: New marine  $\Delta R$   
964 values for Arctic Canada, **Quaternary Geochronology**, 5, 419–434, 2010.

965 [\[19\]](#) Cronin, T.M., Polyak, L., Reed, D., Kandiano, E.S., Marzen, R.E., Council, E.A.: A 600-ka Arctic sea-ice  
966 record from Mendeleev Ridge based on ostracodes, **Quaternary Science Reviews**, 79, 157–167, 2013.

967 [\[20\]](#) Cronin, T.M., DeNinno, L.H., Polyak, L., Caverly, E.K., Poore, R.Z., Brenner, A., Rodriguez-Lazaro, J.,  
968 [Marzen, R.E.: Quaternary ostracode and foraminiferal biostratigraphy and paleoceanography in the](#)  
969 [western Arctic Ocean, \*Marine Micropaleontology\*, 111, 118 - 133 , 2014.](#)  
970 <http://dx.doi.org/10.1016/j.marmicro.2014.05.001>.

971 [\[18\]\[21\]](#) Dalrymple, R.W. and Maass, O. C.: Clay mineralogy of late Cenozoic sediments in the CESAR  
972 cores, Alpha Ridge, central Arctic ocean, **Canadian Journal of Earth Science**, 24, 1562–1569, 1987.

973 [\[19\]\[22\]](#) Darby, D.A.: Kaolinite and other clay minerals in Arctic Ocean sediments, **Journal of**  
974 **Sedimentary Petrology**, 45, 272–279, 1975.

975 [\[20\]\[23\]](#) Darby, D. A., Bischof, J. F., Jones, G. A.: Radiocarbon chronology of depositional regimes in the  
976 western Arctic Ocean, **Deep Sea Research Part II**, 44 (8), 1745–1757, 1997.

---

977 | [\[24\]\[24\]](#) Darby, D. A., Bischof, J. F., Spielhagen, R. F., Marshall, S. A., Herman, S. W.: Arctic ice export  
978 | events and their potential impact on global climate during the Late Pleistocene, **Paleoceanography**,  
979 | 17(2), 1025, doi:10.1029/2001PA000639, 2002.

980 | [\[22\]\[25\]](#) Darby, D. A.: Sources of sediment found in sea ice from the western Arctic Ocean, new insights  
981 | into processes of entrainment and drift patterns, **Journal of Geophysical Research**, 108(C8), 3257,  
982 | doi:10.1029/2002JC001350, 2003.

983 | [\[23\]\[26\]](#) Darby, D. A., and Bischof, J. F.: A Holocene record of changing Arctic Ocean ice drift, analogous  
984 | to the effects of the Arctic Oscillation, **Paleoceanography**, 19, PA1027, doi:10.1029/2003PA000961,  
985 | 2004.

986 | [\[24\]\[27\]](#) Darby, D.A., Polyak, L., Bauch, H.A.: Past glacial and interglacial conditions in the Arctic Ocean  
987 | and marginal seas — a review, **Progress in Oceanography**, 71,129–144, 2006.

988 | [\[25\]\[28\]](#) Darby, D. A., Ortiz, J., Polyak, L., Lund, S., Jakobsson, M., Woodgate, R.A.: The role of currents  
989 | and sea ice in both slowly deposited central Arctic and rapidly deposited Chukchi-Alaskan margin  
990 | sediments, **Global and Planetary Change**, 68, 58-72, 2009.

991 | [\[26\]\[29\]](#) Darby, D. A., Myers, W., Jakobsson, M., Rigor, I.: Modern dirty sea ice characteristics and  
992 | sources: The role of anchor ice, **Journal of Geophysical Research**, 116: C09008,  
993 | doi:10.1029/2010JC006675, 2011.

994 | [\[27\]\[30\]](#) Darby, D., Ortiz, J., Grosch, C., Lund, S.: 1,500-year cycle in the Arctic Oscillation identified in  
995 | Holocene Arctic sea-ice drift. **Nature Geoscience**, 5, 897–900, 2012.

996 | [\[28\]\[31\]](#) Dethleff, D. A., Rachold, V., Tintelnot, T., Antonow, M.: Sea-ice transport of riverine particles  
997 | from the Laptev Sea to Fram Strait based on clay mineral studies, **International Journal of Earth**  
998 | **Science**, 89, 496–502, 2000.

999 | [\[29\]\[32\]](#) Dethleff, D.: Entrainment and export of Laptev Sea ice sediments, Siberian Arctic, **Journal of**  
1000 | **Geophysical Research—Oceans** 110, C07009, doi:10.1029/2004JC002740, 2005.

1001 | [\[30\]\[33\]](#) Dove, D., Polyak, L., Coakley, B.: Widespread, multi-source glacial erosion on the Chukchi  
1002 | margin, Arctic Ocean, **Quaternary Science Reviews**, 92, 112-122, 2014.

1003 | [\[31\]\[34\]](#) Dong, L., Shi, X., Liu, Y., Fang, X., Chen, Z., Wang, C., Zou, J., Huang, Y.: Mineralogical study  
1004 | of surface sediments in the western Arctic Ocean and their implications for material sources, **Advances**  
1005 | **in Polar Science**, 25(3),192-203, 2014.

1006 | [\[32\]\[35\]](#) Dowdeswell, J. A., Villinger, H., Whittington, R. J., Marienfeld, P.: Iceberg scouring in Scoresby  
1007 | Sund and on the East Greenland continental shelf, **Marine Geology**, 111, 37–53, 1993.

- 
- 1008 | [\[33\]\[36\]](#) Dyke, A. S., Andrews, J. T., Clark, P. U., England, J. H., Miller, G. H., Shaw, J., Veillette, J. J.:  
1009 | The Laurentide and Innuitian ice sheets during the Last Glacial Maximum, **Quaternary Science Review**,  
1010 | 21, 9–31, 2002.
- 1011 | [\[34\]\[37\]](#) England, J.H., Furze, M.F.A., Doupé, J.P.: Revision of the NW Laurentide Ice Sheet: implications  
1012 | for paleoclimate, the northeast extremity of Beringia, and Arctic Ocean sedimentation, **Quaternary**  
1013 | **Science Review**, 28, 1573-1596, 2009.
- 1014 | [\[38\]](#) Fagel, N., Not, C., Gueibe, J., Mattielli, N., Bazhenova, E.: Late Quaternary evolution of sediment  
1015 | provenances in the Central Arctic Ocean: mineral assemblage, trace element composition and Nd and Pb  
1016 | isotope fingerprints of detrital fraction from the Northern Mendeleev Ridge, **Quaternary Science**  
1017 | **Reviews**, 92, 140-154, 2014.
- 1018 | [\[35\]\[39\]](#) Grosswald, M.G.: An ice sheet on the East Siberian shelf in the late Pleistocene. In: **The**  
1019 | **Pleistocene of Siberia. Stratigraphy and interregional correlations.** Novosibirsk, Nauka, Sibirskoye  
1020 | otdeleniye, pp. 48–57, 1989.
- 1021 | [\[36\]\[40\]](#) Grosswald, M.G. and Hughes, T.J.: The Russian component of an Arctic Ice Sheet during the Last  
1022 | Glacial Maximum, **Quaternary Science Review**, 21, 121-146, 2002.
- 1023 | [\[37\]\[41\]](#) Haley, B.A. and Polyak, L.: Pre-modern Arctic Ocean circulation from surface sediment  
1024 | neodymium isotopes, **Geophysical Research Letters**, 40, 1–5, 2013.
- 1025 | [\[38\]\[42\]](#) Hanslik, D., Jakobsson, M., Backman, J., Björck, S., Sellén, E., O'Regan, M., Fornaciari, E., Skog,  
1026 | G.: Quaternary Arctic Ocean sea ice variations and radiocarbon reservoir age corrections, **Quaternary**  
1027 | **Science Reviews**, 29, 3430–3441, 2010.
- 1028 | [\[43\]](#) Harrison, J.C., St-Onge, M.R., Petrov, O., Strelnikov, S., Lopatin, B., Wilson, F., Tella, S., Paul, D.,  
1029 | Lynds, T., Shokalsky, S., Hults, C., Bergman, S., Jepsen, H.F., Solli, A.: **Geological Map of the Arctic.**  
1030 | Geol. Survey Canada, p. 5816. Open File, 2008.
- 1031 | [\[39\]\[44\]](#) Head, M.J. and Gibbard, P.L.: Early-Middle Pleistocene transitions: linking terrestrial and marine  
1032 | realms, **Quaternary International**, 389, 7-46, 2015.
- 1033 | [\[40\]\[45\]](#) Hebbeln, D.: Flux of ice-rafted detritus from sea ice in the Fram Strait, **Deep-Sea Research**  
1034 | **Part II**, 47, 1773–1790, 2000.
- 1035 | [\[41\]\[46\]](#) Hesse, R. and Khodabakhsh, S.: Anatomy of Labrador Sea Heinrich layers, **Marine Geology**, 380,  
1036 | 44–66, 2016.
- 1037 | [\[42\]\[47\]](#) Hughes, T.J., Denton, G.H., Grosswald, M.G.: Was there a late-Würm Arctic ice sheet? **Nature**,

1038 266, 596-602, 1977.

1039 [\[48\]](#) Ivanova, V.V.: Geochemical features of formation of massive ground ice bodies (New Siberian Island,  
1040 Siberian Arctic) as the evidence of their genesis. *Earth's Cryosphere*, 16, 56–70, 2012 (in Russian).

1041 [\[43\]](#)[\[49\]](#) Jakobsson, M., Løvlie, R., Al-Hanbali, H., Arnold, E., Backman, J., Mörth, M.: Manganese and  
1042 color cycle in Arctic Ocean sediments constrain Pleistocene chronology, *Geology*, 28, 23–26, 2000.

1043 [\[44\]](#)[\[50\]](#) Jakobsson, M., Polyak, L., Edwards, M., Kleman, J., Coakley, B.: Glacial geomorphology of the  
1044 Central Arctic Ocean: the Chukchi Borderland and the Lomonosov Ridge, *Earth Surface Processes and*  
1045 *Landforms*, 33, 526–545, 2008.

1046 [\[45\]](#)[\[51\]](#) Jakobsson, M., Andreassen, K., Bjarnadóttir, L. R., Dove, D., Dowdeswell, J. A., England, J.H.,  
1047 Funder, S., Hogan, K., Ingólfsson, Ó., Jennings, A., Larsen, N. K., Kirchner, N., Landvik, J.Y., Mayer, L.,  
1048 Mikkelsen, N., Möller, P., Niessen, F., Nilsson, J., O'Regan, M., Polyak, L., Nørgaard-Pedersen, N.,  
1049 Stein, R.: Arctic Ocean glacial history, *Quaternary Science Reviews*, 92, 40–67, 2014.

1050 [\[46\]](#)[\[52\]](#) Jakobsson, M., Nilsson, J., Anderson, L., Backman, J., Björk, G., Cronin, T.M., Kirchner, N.,  
1051 Koshurnikov, A., Mayer, L., Noormets, R., O'Regan, M., Stranne, C., Ananiev, R., Macho, N. B.,  
1052 Cherniykh, D., Coxall, H., Eriksson, B., Flodén, T., Gemery, L., Gustafsson, O., Jerram, K., Johansson, C.,  
1053 Khortov, A., Mohammad, R., Semiletov, I.: Evidence for an ice shelf covering the central Arctic Ocean  
1054 during the penultimate glaciation, *Nature Communications*, doi: 10.1038/ncomms10365, 2016.

1055 [\[47\]](#)[\[53\]](#) Jang, K., Han, Y., Huh, Y., Nam, S., Stein, R., Mackensen, A., Matthiessen, J.: Glacial freshwater  
1056 discharge events recorded by authigenic neodymium isotopes in sediments from the Mendeleev Ridge,  
1057 western Arctic Ocean, *Earth and Planetary Science Letters*, 369-370, 148–157, 2013.

1058 [\[48\]](#)[\[54\]](#) Junttila, J.: Clay minerals in response to Mid-Pliocene glacial history and climate in the polar  
1059 regions (ODP, Site 1165, Prydz Bay, Antarctica and Site 911, Yermak Plateau, Arctic Ocean), *Acta*  
1060 *Universitat Ouluensis*, A 481, 2007.

1061 [\[49\]](#)[\[55\]](#) Kalinenko, V.V.: Clay minerals in sediments of the Arctic Seas. *Lithology and Mineral*  
1062 *Resources*, 36, 362–372, 2001.

1063 [\[50\]](#)[\[56\]](#) Kaparulina, E., Strand, K., Lunkka, J. P.: Provenance analysis of central Arctic Ocean sediments:  
1064 Implications for circum-Arctic ice sheet dynamics and ocean circulation during Late Pleistocene,  
1065 *Quaternary Science Reviews*, 147, 210-220, 2016.

1066 [\[51\]](#)[\[57\]](#) Keigwin, L.D., Donnelly, J.P., Cook, M.S., Driscoll, N.W., Brigham-Grette, J.: Rapid sea-level  
1067 rise and Holocene climate in the Chukchi Sea, *Geology*, 34 (10), 861–864, doi:10.1130/G22712.1, 2006.

- 1068 | [\[52\]\[58\]](#) Kim, B.I. and Slobodin, V.Ya.: Main stages of the evolution of East Arctic shelves of Russia and  
1069 | Canadian Arctic in the Paleogene and Neogene, **In: Geologiya skladchatogo obramleniya**  
1070 | **Ameraziiskogo subbasseina (Geology of the Folded Framing of the Amerasian Subbasin)**, St.  
1071 | Petersburg: Sevmorgeologiya, 104–116, 1991.
- 1072 | [\[53\]\[59\]](#) Knies, J., Kleiber, H. P., Matthiessen, J., Müller, C., Nowaczyk, N.: Marine ice-rafted debris  
1073 | records constrain maximum extent of Saalian and Weichselian ice-sheets along the northern Eurasian  
1074 | margin, **Global and Planetary Change**, 31, 45–64, 2001.
- 1075 | [\[54\]\[60\]](#) Knies, J. and Vogt, C.: Freshwater pulses in the eastern Arctic Ocean during Saalian and early  
1076 | Weichselian ice-sheet collapse, **Quaternary Research**, 60, 243–251, 2003.
- 1077 | [\[55\]\[61\]](#) Kobayashi, D., Yamamoto, M., Tirino, T., Nam, S.-I., Park, Y.-H., Harada, N., Nagashima, K.,  
1078 | Chikita, K., Saitoh, S.I.: Distribution of detrital minerals and sediment color in western Arctic Ocean and  
1079 | northern Bering Sea sediments: changes in the provenance of western Arctic Ocean sediments since the  
1080 | last glacial period, **Polar Science**, 10, 519–531, 2016.
- 1081 | [\[56\]\[62\]](#) Krylov, A. A., Andreeva I. A., Vogt C., Backman J., Krupskaya V. V., Grikurov G. E., Moran K.,  
1082 | Shoji H.: A shift in heavy and clay mineral provenance indicates a middle Miocene onset of a perennial  
1083 | sea ice cover in the Arctic Ocean, **Paleoceanography**, 23, PA1S06, doi:10.1029/2007PA001497, 2008.
- 1084 | [\[57\]\[63\]](#) Krylov, A.A., Stein, R., Ermakova, L.A. Clay minerals as indicators of late quaternary  
1085 | sedimentation constraints in the Mendeleev Rise, Amerasian Basin, Arctic Ocean, **Lithology and**  
1086 | **Mineral Resources**, 49, 103-116, 2014.
- 1087 | [\[58\]\[64\]](#) Larsen, E., Kjær, K.H., Demidov, I.N., Funder, S., Grøsfjeld, K., Houmark-Nielsen, M., Jensen,  
1088 | M., Linge, H., Lyså, A.: Late Pleistocene glacial and lake history of northwestern Russia, **Boreas**, 35,  
1089 | 394-424 , 2006.
- 1090 | [\[59\]\[65\]](#) Lazar, K.B. and Polyak, L.: Pleistocene benthic foraminifers in the Arctic Ocean: Implications for  
1091 | seaice and circulation history, **Marine Micropaleontology**, 126, 19-30, 2016.
- 1092 | [\[66\]](#) Löwemark, L., Jakobsson, M., Mörth, M., Backman, J.: Arctic Ocean Mn contents and sediment colour  
1093 | cycles. **Polar Research**, 27, 105–113, 2008.
- 1094 | [\[60\]\[67\]](#) Löwemark, L., März, C., O'Regan, M., Gyllencreutz, R. Arctic Ocean Mn-stratigraphy: genesis,  
1095 | synthesis and inter-basin correlation, **Quaternary Science Reviews**, 92, 97-111, 2014.
- 1096 | [\[64\]\[68\]](#) Margold M., Stokes C. R., Clark C. D.: Ice streams in the Laurentide Ice Sheet: Identification,  
1097 | characteristics and comparison to modern ice sheets, **Earth-Science Reviews**, 143, 117–146, 2015.



- 
- 1098 | [\[62\]\[69\]](#) März, C., Stratmann, A., Matthiessen, J., Meinhardt, A., Eckert, S., Schnetger, B., Vogt, C., Stein,  
1099 | R., Brumsack, H.: Manganese-rich brown layers in Arctic Ocean sediments: composition, formation  
1100 | mechanisms, and diagenetic overprint, **Geochimica et Cosmochimica Acta**, 75, 7668–7687, 2011.
- 1101 | [\[63\]\[70\]](#) Matthiessen, J., Niessen F., Stein, R., Naafs, B. D.: Pleistocene Glacial Marine Sedimentary  
1102 | Environments at the Eastern Mendeleev Ridge, Arctic Ocean, **Polarforschung**, 79 (2), 123 – 137, 2009  
1103 | (erschienen 2010).
- 1104 | [\[64\]\[71\]](#) Naidu, A.S., Burrell, D.C., Hood, D.W.: Clay mineral composition and geological significance of  
1105 | some Beaufort Sea sediments, **Journal of Sedimentary Petrology**, 41, 691–694, 1971.
- 1106 | [\[65\]\[72\]](#) Naidu, A. S., Creager, J. S., Mowatt, T. C.: Clay mineral dispersal patterns in the north Bering  
1107 | and Chukchi Seas. **Marine Geology**, 47(1), 1-15, 1982.
- 1108 | [\[66\]\[73\]](#) Niessen, F., Hong, J.K., Hegewald, A., Matthiessen, J., Stein, R., Kim, H., Kim, S., Jensen, L.,  
1109 | Jokat, W., Nam, S.-I., Kang, S.-H.: Repeated Pleistocene glaciation of the East Siberian Continental  
1110 | Margin, **Nature Geoscience**, 6, 842-846, 2013.
- 1111 | [\[67\]\[74\]](#) Nürnberg, D., Wollenburg, I., Dethleff, D., Eicken, H., Kassens, H., Letzig, T., Reimnitz, E.,  
1112 | Thiede, J.: Sediments in Arctic sea ice: Implications for entrainment, transport and release, **Marine**  
1113 | **Geology**, 119, 185–214, 1994.
- 1114 | [\[68\]\[75\]](#) Nwaodua, E.C., Ortiz J. D., Griffith E. M.: Diffuse spectral reflectance of surficial sediments  
1115 | indicates sedimentary environments on the shelves of the Bering Sea and western Arctic, **Marine**  
1116 | **Geology**, 355, 218–233, 2014.
- 1117 | [\[76\]](#) [Okulitch, A.V. \(compiler\): Geology of the Canadian Archipelago and North Greenland. In: Trettin,](#)  
1118 | [H.P. \(Ed.\), Innuitian orogen and Arctic Platform: Canada and Greenland. The Geology of North America.](#)  
1119 | [The Geological Society of America, Boulder, Colorado, E, 1:200,000, 1991.](#)
- 1120 | [\[69\]\[77\]](#) O'Regan, M., King, J., Backman, J., Jakobsson, M., Pälike, H., Moran, K., Heil, C., Sakamoto,  
1121 | T., Cronin, T.M., Jordan, R.W.: Constraints on the Pleistocene chronology of sediments from the  
1122 | Lomonosov Ridge, **Paleoceanography**, 23, PA1S19, doi:10.1029/2007PA001551 , 2008.
- 1123 | [\[70\]\[78\]](#) Ortiz, J.D., Polyak, L., Grebmeier, J.M., Darby, D., Eberl, D.D., Naidu, S., Nof, D.: Provenance  
1124 | of Holocene sediment on the Chukchi–Alaskan margin based on combined diffuse spectral reflectance  
1125 | and quantitative X-Ray diffraction analysis, **Global and Planetary Change**, 68 (no. 1–2), 73–84, 2009.
- 1126 | [\[79\]](#) [Pelto, B.M.: Sedimentological, geochemical and isotopic evidence for the establishment of modern](#)  
1127 | [circulation through the Bering Strait and depositional environment history of the Bering and Chukchi](#)

---

1128 [seas during the last deglaciation. \*\*Master Thesis\*\*, University of Massachusetts – Amherst, Paper 108, 134](#)  
1129 [pp., 2014 \(http://scholarworks.umass.edu/masters\\_theses\\_2/108\).](http://scholarworks.umass.edu/masters_theses_2/108)

1130 [\[74\]\[80\]](#) Phillips, R. L. and Grantz, A.: Regional variations in provenance and abundance of ice-rafted  
1131 clasts in Arctic Ocean sediments: Implications for the configuration of late Quaternary oceanic and  
1132 atmospheric circulation in the Arctic, **Marine Geology**, 172, 91–115, 2001.

1133 [\[72\]\[81\]](#) Poirier, R.K., Cronin, T.M., Briggs Jr., W.M., Lockwood, R.: Central Arctic paleoceanography for  
1134 the last 50 kyr based on ostracode faunal assemblages, **Marine Micropaleontology**, 88–89, 65–76, 2012.

1135 [\[73\]\[82\]](#) Polyak, L., Edwards, M.H., Coakley, B.J., Jakobsson, M.: Ice shelves in the Pleistocene Arctic  
1136 Ocean inferred from glaciogenic deep-sea bedforms, **Nature**, 410, 453–459, 2001.

1137 [\[74\]\[83\]](#) Polyak, L., Curry, W. B., Darby, D. A., Bischof, J., Cronin, T. M.: Contrasting glacial/interglacial  
1138 regimes in the Western Arctic Ocean as exemplified by a sedimentary record from the Mendeleev Ridge,  
1139 **Palaeogeography, Palaeoclimatology, Palaeoecology**, 203, 73–93, 2004.

1140 [\[75\]\[84\]](#) Polyak, L., Darby, D.A., Bischof, J., Jakobsson, M.: Stratigraphic constraints on late Pleistocene  
1141 glacial erosion and deglaciation of the Chukchi margin, Arctic Ocean, **Quaternary Research**,  
1142 67:234–245, doi:10.1016/j.yqres.2006.08.001, 2007.

1143 [\[76\]\[85\]](#) Polyak, L., Bischof, J., Ortiz, J.D., Darby, D.A., Channell, J.E.T., Xuan, C., Kaufman, D.S.,  
1144 Lovlie, R., Schneider, D.A., Eberl, D.D., Adler, R.E., Council, E.A.: Late Quaternary stratigraphy and  
1145 sedimentation patterns in the western Arctic Ocean, **Global and Planetary Change**, 68, 5-17, 2009.

1146 [\[77\]\[86\]](#) Polyak, L., Alley, R.B., Andrews, J.T., Brigham-Grette, J., Cronin, T.M., Darby, D.A., Dyke, A.S.,  
1147 Fitzpatrick, J.J., Funder, S., Holland, M., Jennings, A.E., Miller, G.H., O’Regan, M., Savelle, J., Serreze,  
1148 M., St. John, K., White, J.W.C., Wolff, E.: History of sea ice in the Arctic, **Quaternary Science Reviews**,  
1149 29, 1757-1778, 2010.

1150 [\[78\]\[87\]](#) Polyak, L., Best, K. M., Crawford, K. A., Council, E. A., St-Onge, G.: Quaternary history of sea  
1151 ice in the western Arctic Ocean based on foraminifera, **Quaternary Science Reviews**, 79, 145-156, 2013.

1152 [\[79\]\[88\]](#) Ramaswamy V. and Rao P. S.: Grain Size Analysis of Sediments from the Northern Andaman Sea:  
1153 Comparison of Laser Diffraction and Sieve-Pipette Techniques, **Journal of Coastal Research**, 22,  
1154 1000–1009, 2006.

1155 [\[80\]\[89\]](#) Rigor, I.G., Wallace, J.M., Colony, R.L.: Response of sea ice to the Arctic Oscillation, **Journal of**  
1156 **Climate**, 15, 2648–2663, 2002.

- 1157 | [\[84\]\[90\]](#) Rudels, B.: Arctic Ocean circulation. **Encyclopedia of Ocean Sciences**, J.H. Steele, K.K.  
1158 | Turekian, S.A. Thorpe (Eds.-in-Chief), Elsevier, 211-225, 2009.
- 1159 | [\[82\]\[91\]](#) Sharma, M., Basu, A.R., Nesterenko, G. V.: Temporal Sr-, Nd- and Pb isotopic variations in the  
1160 | Siberian flood basalts: implications for the plume-source characteristics, **Earth and Planetary Science**  
1161 | **Letters**, 113, 365-381, 1992.
- 1162 | [\[92\]](#) Simon, Q., Hillaire-Marcel, C., St-Onge, G., Andrews, J.: North-eastern Laurentide, western Greenland  
1163 | and southern Innuitian ice stream dynamics during the last glacial cycle, **Journal of Quaternary**  
1164 | **Science**, 29, 14–26, 2014.
- 1165 | [\[83\]\[93\]](#) Slobodin, V.Ya., Kim, B.I., Stepanova, G.V., Kovalenko, F.Ya.: Differentiation of the Aion  
1166 | borehole section based on the biostratigraphic data, In: **Stratigrafiya i paleontologiya mezo-kainozoya**  
1167 | **Sovetskoi Arktiki (Stratigraphy and Paleontology of the Meso-Cenozoic in the Soviet Arctic)**,  
1168 | Leningrad: Sevmorgeologiya, 43–58, 1990.
- 1169 | [\[84\]\[94\]](#) Spielhagen, R. F., Bonani, G., Eisenhauer, A., Frank, M., Frederichs, T., Kassens, H., Kubik, P.  
1170 | W., Mangini, A., Nørgaard-Pedersen, N., Nowaczyk, N. R., Schäper, S., Stein, R., Thiede, J., Tiedemann,  
1171 | R., Wabsner, M.: Arctic Ocean evidence for Late Quaternary initiation of northern Eurasian ice  
1172 | sheets, **Geology**, 25, 783–786, 1997.
- 1173 | [\[85\]\[95\]](#) Spielhagen, R. F., Baumann, K. H., Erlenkeuser, H., Nowaczyk, N. R., Nørgaard-Pedersen,  
1174 | N., Vogt, C., Weiel, D. Arctic Ocean deep-sea record of Northern Eurasian ice sheet history, **Quaternary**  
1175 | **Science Review**, 23, 1455–1483, 2004.
- 1176 | [\[86\]\[96\]](#) Schoster, F., Behrends, M., Müller, C., Stein, R., Wabsner, M.: Modern river discharge in the  
1177 | Eurasian Arctic Ocean: Evidence from mineral assemblages and major and minor element distributions,  
1178 | **International Journal of Earth Science**, 89, 486–495, 2000.
- 1179 | [\[87\]\[97\]](#) Sellén, E., O'Regan, M., Jakobsson, M.: Spatial and temporal Arctic Ocean depositional regimes:  
1180 | a key to the evolution of ice drift and current patterns, **Quaternary Science Reviews**, 29, 3644-3664,  
1181 | 2010.
- 1182 | [\[88\]\[98\]](#) Stärz, M., Gong, X., Stein, R., Darby, D.A., Kauker, F., Lohmann, G.: Glacial shortcut of Arctic  
1183 | sea-ice transport, **Earth and Planetary Science Letters**, 357–358, 257–267, 2012.
- 1184 | [\[89\]\[99\]](#) Stein, R., Grobe, H., Wabsner, M.: Organic carbon, carbonate, and clay mineral distributions in  
1185 | eastern central Arctic Ocean surface sediments, **Marine Geology**, 119, 269-285, 1994.
- 1186 | [\[90\]\[100\]](#) Stein R.: Arctic Ocean Sediments: Processes, Proxies, and Paleoenvironment, **Elsevier**,

---

1187 Amsterdam, 1-592 pp, 2008.

1188 [\[94\]\[101\]](#) Stein, R., Matthiessen, J., Niessen, F.: Re-Coring at Ice Island T3 Site of Key Core FL-224  
1189 (Nautilus Basin, Amerasian Arctic): Sediment Characteristics and Stratigraphic Framework,  
1190 **Polarforschung**, 79 (2), 81 – 96, 2010a.

1191 [\[92\]\[102\]](#) Stein, R., Matthiessen, J., Niessen, F., Krylov, A., Nam, S., Bazhenova, E., Shipboard Geology  
1192 Group.: Towards a better (litho-) stratigraphy and reconstruction of Quaternary paleoenvironment in the  
1193 Amerasian Basin (Arctic Ocean), **Polarforschung**, 79 (2), 97–121, 2010b.

1194 [\[93\]\[103\]](#) Stein, R., Fahl, K., Müller J.: Proxy Reconstruction of Cenozoic Arctic Ocean Sea-Ice History–  
1195 from IRD to IP25, **Polarforschung**, 82 (1), 37–71, 2012.

1196 [\[94\]\[104\]](#) Stokes, C.R., Clark, C.D., Darby, D., Hodgson, D.A.: Late Pleistocene ice export events into the  
1197 Arctic Ocean from the M'Clure Strait Ice Stream, Canadian Arctic Archipelago, **Global and Planetary**  
1198 **Change**, 49, 139–162, 2005.

1199 [\[95\]\[105\]](#) Stokes, C.R., Clark, C.D., Storrar, R.: Major changes in ice stream dynamics during deglaciation  
1200 of the north-western margin of the Laurentide Ice Sheet, **Quaternary Science Reviews**, 28, 721-738,  
1201 2009.

1202 [\[96\]\[106\]](#) Svendsen, J. I., Alexanderson, H., Astakhov, V. I., Demidov, I., Dowdeswell, J. A., Funder,  
1203 S., Gataullin, V., Henriksen, M., Hjort, C., Houmark-Nielsen, M., Hubberten, H. W., Ingólfsson, O.,  
1204 Jakobsson, M., Kjær, K. H., Larsen, E., Lokrantz, H., Lunkka, J. P., Lyså, A., Mangerud, J., Matioushkov,  
1205 A., Murray, A., Möller, P., Niessen, F., Nikolskaya, O., Polyak, L., Saarnisto, M., Siegert, R., Siegert, M.  
1206 J., Spielhagen, R. F., Stein, R.: Late Quaternary ice sheet history of Northern Eurasia, **Quaternary**  
1207 **Science Review**, 23, 1229–1271, 2004.

1208 [\[97\]\[107\]](#) Vogt, C.: Regional and temporal variations of mineral assemblages in Arctic Ocean sediments as  
1209 climatic indicator during glacial/interglacial changes, **Report on Polar Marine Research**, 251, 309,  
1210 1997.

1211 [\[98\]\[108\]](#) Vogt, C., Knies, J., Spielhagen, R. F., Stein, R.: Detailed mineralogical evidence for two nearly  
1212 identical glacial/deglacial cycles and Atlantic water advection to the Arctic Ocean during the last 90,000  
1213 years, **Global and Planetary Change**, 31, 23–44, 2001.

1214 [\[99\]\[109\]](#) Vogt, C. and Knies, J.: Sediment dynamics in the Eurasian Arctic Ocean during the last  
1215 deglaciation — The clay mineral group smectite perspective, **Marine Geology**, 250, 211–222, 2008.

- 
- 1216 | [\[100\]\[110\]](#) Vogt, C. and Knies, J.: Sediment pathways in the western Barents Sea inferred from clay mineral  
1217 | assemblages in surface sediments, **Norwegian Journal of Geology**, 89, 41–55, 2009.
- 1218 | [\[101\]\[111\]](#) Viscosi-Shirley, C., Mammone, K., Pisias, N., Dymond, J.: Clay mineralogy and multi-element  
1219 | chemistry of surface sediments on the Siberian-Arctic shelf: Implications for sediment provenance and  
1220 | grain size sorting, **Continental Shelf Research**, 23, 1175–1200, 2003.
- 1221 | [\[102\]\[112\]](#) Wahsner, M., Müller, C., Stein, R., Ivanov, G., Levitan, M., Shelekova, E., Tarasov, G.: Clay  
1222 | mineral distributions in surface sediments from the Central Arctic Ocean and the Eurasian continental  
1223 | margin as indicator for source areas and transport pathways: a synthesis, **Boreas**, 28, 215-233, 1999.
- 1224 | [\[103\]\[113\]](#) Wang, D. and Hesse, R.: Continental slope sedimentation adjacent to an ice-margin. II.  
1225 | Glaciomarine depositional facies on Labrador Slope and glacial cycles, **Marine Geology**, 135, 65-96,  
1226 | 1996.
- 1227 | [\[104\]\[114\]](#) Wang, R., Xiao, W., März, C., Li, Q.: Late Quaternary paleoenvironmental changes revealed by  
1228 | multi-proxy records from the Chukchi Abyssal Plain, western Arctic Ocean, **Global and Planetary**  
1229 | **Change**, 108, 100–118, 2013.
- 1230 | [\[105\]\[115\]](#) Winkler, A., Wolf-Welling, T.C.W., Statterger, K., Thiede, J.: Clay mineral sedimentation in high  
1231 | northern latitude deep-sea basins since the Middle Miocene (ODP Leg 151, NAAG), **International**  
1232 | **Journal of Earth Sciences**, 91,133–148, 2002.
- 1233 | [\[106\]\[116\]](#) Winter, B.L., Johnson, C.M., Clark, D.L.: Strontium, neodymium, and lead isotope variations of  
1234 | authigenic and silicate sediment components from the Late Cenozoic Arctic Ocean: implications for  
1235 | sediment provenance and the source of trace metals in seawater, **Geochimica et Cosmochimica Acta**, 61,  
1236 | 4181-4200, 1997.
- 1237 | [\[107\]\[117\]](#) Xiao, W., Wang, R., Polyak, L., Astakhov, A., Cheng, X.: Stable oxygen and carbon isotopes in  
1238 | planktonic foraminifera *Neogloboquadrina pachyderma* in the Arctic Ocean: an overview of published  
1239 | and new surface-sediment data, **Marine Geology**, 352, 397-408, 2014.
- 1240 | [\[108\]\[118\]](#) Xuan, C. and Channell, J.E.T.: Origin of apparent magnetic excursions in deep-sea sediments  
1241 | from Mendeleev-Alpha Ridge (Arctic Ocean), **Geochemistry, Geophysics, Geosystems**, 11, Q02003,  
1242 | 2010.
- 1243 | [\[109\]\[119\]](#) Yurco, L. N., Ortiz, J. D., Polyak, L., Darby, D. A., Crawford, K. A.: Clay mineral cycles  
1244 | identified by diffuse spectral reflectance in Quaternary sediments from the Northwind Ridge:  
1245 | implications for glacial–interglacial sedimentation patterns in the Arctic Ocean, **Polar Research**, 29,

- 
- 1246 176–197, 2010.
- 1247 [\[120\]](#) Zou, H.: An X-ray diffraction approach: bulk mineral assemblages as provenance indicator of sediments
- 1248 from the Arctic Ocean, **PhD Thesis**, University of Bremen, Bremen, 1-104 pp, 2016.
- 1249 

---

1250 **Table 1.** Minerals Actively Sought in Diffraction Data Analysis

1251

Mineral	Window(°2θ, CuKα radiation)	Range of D-Spacing(A)	Intensity Factor*
Amphibole	10.30-10.70	8.59- 8.27	2.5
Augite	29.70-30.00	3.00- 2.98	5
Calcite	29.25-29.60	3.04- 3.01	1.65
Chlorite	18.50-19.10	4.79_ 4.64	4.95
Dolomite	30.80-31.15	2.90- 2.87	1.53
K-Feldspar	27.35-27.79	3.26- 3.21	4.3
Quartz	26.45-26.95	3.37- 3.31	1

1252

\*The intensity factors are determined in 1:1 mixtures with quartz by obtaining the ratio of the diagnostic peak intensity of each mineral with that of quartz, which is assigned a value of 1.00. The detection limit in weight percent of the minerals in a siliceous or calcareous matrix can be obtained by multiplying the intensity factor by 0.12 (Cook, 1975) .

1253

1254

1255

1256

1257

**Table 2.** AMS<sup>14</sup>C datings in core BN05

Sample no.	Depth (cm)	AMS 14C age(14C a BP)	Calibrated age median (cal yr BP)	2-σ range (cal yr BP)
112767	4-6	7810±35	7885	7797-7958
112768	8-10	8180±35	8259	8171-8340
112769	18-20	38600±300	41703	41202-42165
115944	22-24	40800±410	43140	42522-43901

1258

**Table S43.** Loading scores for variables used in the PCA

	PC1	PC2	PC3	PC4	PC5
<u>% of Variance</u>	<u>18.94</u>	<u>17.27</u>	<u>15.71</u>	<u>14.78</u>	<u>10.05</u>
<u>Ca/Al</u>	<u>0.18</u>	<u>-0.07</u>	<u><b>0.62</b></u>	<u><b>0.57</b></u>	<u>0.18</u>
<u>Mn/Al</u>	<u><b>0.75</b></u>	<u>-0.18</u>	<u>-0.10</u>	<u>0.03</u>	<u>-0.20</u>
<u>Clay (%)</u>	<u><b>0.77</b></u>	<u>-0.44</u>	<u>0.03</u>	<u>-0.19</u>	<u>-0.25</u>
<u>Silt (%)</u>	<u>-0.80</u>	<u>0.17</u>	<u>-0.13</u>	<u>0.07</u>	<u>-0.41</u>
<u>Fine sand(%)</u>	<u>-0.34</u>	<u><b>0.50</b></u>	<u>0.02</u>	<u>0.21</u>	<u><b>0.64</b></u>
<u>&gt;250 μm (%)</u>	<u>-0.19</u>	<u>0.12</u>	<u>0.26</u>	<u>0.09</u>	<u><b>0.86</b></u>
<u>Plankt. Foram. (% &gt;63 μm)</u>	<u><b>0.78</b></u>	<u>-0.06</u>	<u>-0.06</u>	<u>0.04</u>	<u>-0.34</u>
<u>Smectite (%)</u>	<u>-0.18</u>	<u><b>0.80</b></u>	<u>0.05</u>	<u>-0.11</u>	<u>-0.10</u>
<u>Illite (%)</u>	<u>0.17</u>	<u><b>-0.96</b></u>	<u>0.04</u>	<u>0.03</u>	<u>-0.17</u>
<u>Kaolinite (%)</u>	<u>-0.17</u>	<u><b>0.76</b></u>	<u>0.13</u>	<u>0.07</u>	<u>0.41</u>
<u>Chlorite (%)</u>	<u>-0.01</u>	<u><b>0.70</b></u>	<u>-0.42</u>	<u>-0.07</u>	<u>-0.01</u>

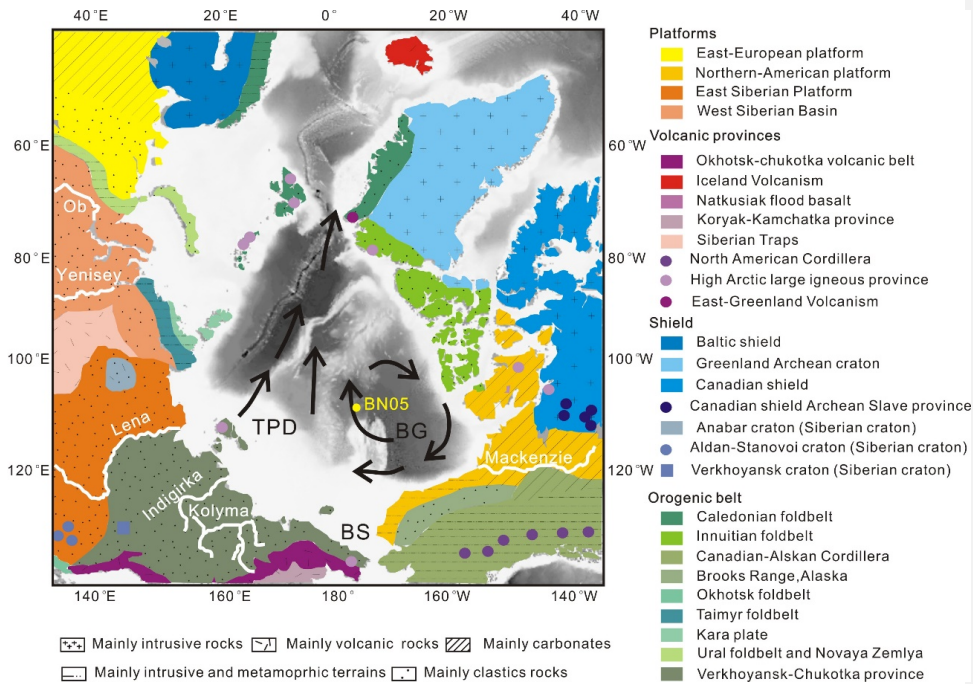
Quartz (%)	<u>-0.30</u>	<u>0.18</u>	<u>-0.47</u>	<u>-0.08</u>	<u>-0.04</u>
K-feldspar (%)	<u>-0.03</u>	<u>0.16</u>	<u>-0.02</u>	<b><u>-0.91</u></b>	<u>0.07</u>
Plagioclase (%)	<u>-0.15</u>	<u>0.09</u>	<b><u>-0.78</u></b>	<u>-0.48</u>	<u>-0.12</u>
Calcite (%)	<b><u>0.87</u></b>	<u>-0.05</u>	<u>0.07</u>	<u>0.27</u>	<u>-0.05</u>
Pyroxene (%)	<u>-0.11</u>	<u>-0.18</u>	<u>-0.28</u>	<b><u>-0.69</u></b>	<u>-0.27</u>
Dolomite (%)	<u>-0.05</u>	<u>-0.12</u>	<b><u>0.72</u></b>	<b><u>0.56</u></b>	<u>0.15</u>
Qz/Fsp	<u>-0.12</u>	<u>0.06</u>	<u>0.28</u>	<b><u>0.66</u></b>	<u>0.10</u>
Kfsp/Plag	<u>-0.11</u>	<u>0.05</u>	<b><u>0.89</u></b>	<u>-0.05</u>	<u>0.11</u>

Scores >0.5 (<-0.5) are highlighted in bold.

**Table 3.** Characterization and interpretation of sedimentary variable groups (Fig. 6)

Group	Leading/opposite proxies	Environments	Depositional processes	Provenance
1	Foraminifers, calcite, Mn, clay/coarse grains (esp. silt), quartz	Interglacial (incl. major interstadials)	Sea ice	Mixed
2	Dolomite, Ca, Qua/Fsp/plagioclase, pyroxene, feldspar	Glacial/ deglacial	Icebergs, meltwater	North-American
3	Feldspar, pyroxene, plagioclase/ Ca, dolomite, Qua/Fsp	Interglacial/ deglacial	Sea ice, icebergs	Siberian
4	Smectite, kaolinite, chlorite/ clay	Glacial/ deglacial	Icebergs, debris flows	E-Siberian
5,6	Coarse grains (incl. silt)	Glacial/ deglacial	Icebergs, debris flows	Mixed





1265

1266

1267 **Figure 1.** Background map showing the location of core ARC4-BN05, the main Arctic

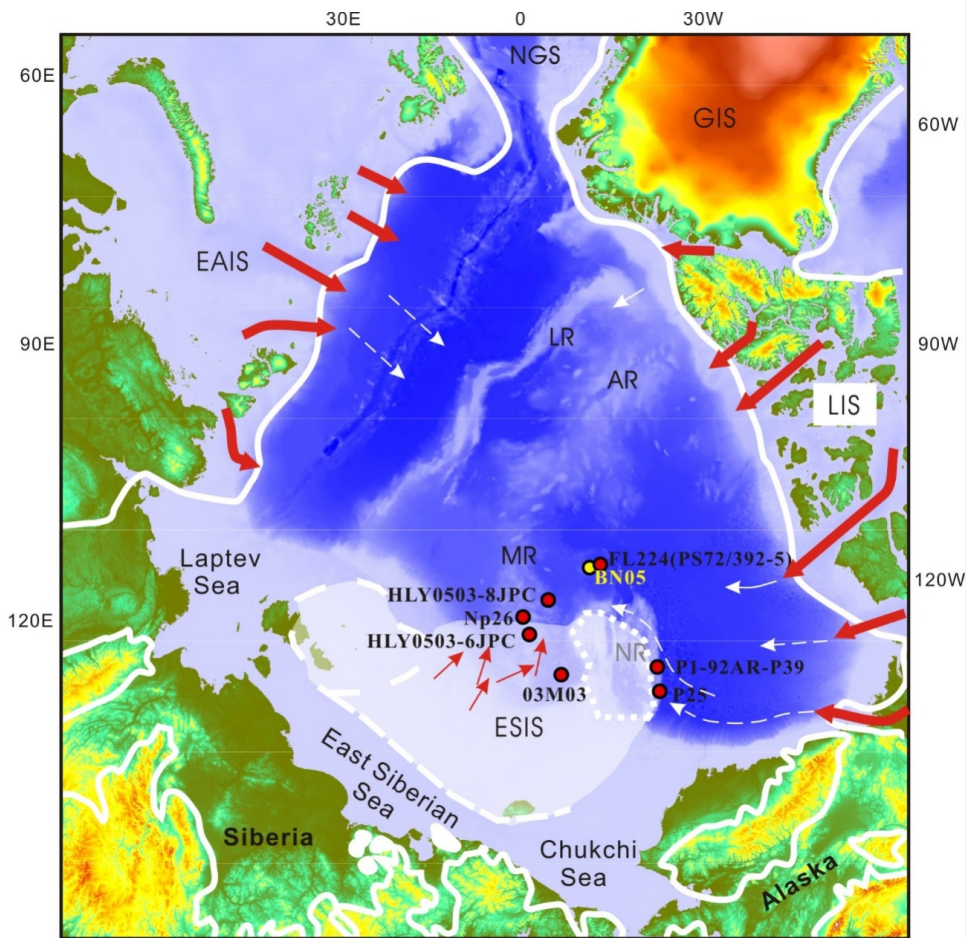
1268 rivers and the two major surface current systems: Beaufort Gyre (BG) and Transpolar

1269 Drift (TPD). Schematic geological map shows the distribution and prevailing

1270 lithology of the main terrains adjacent to the Arctic Ocean (Fagel et al., 2014).

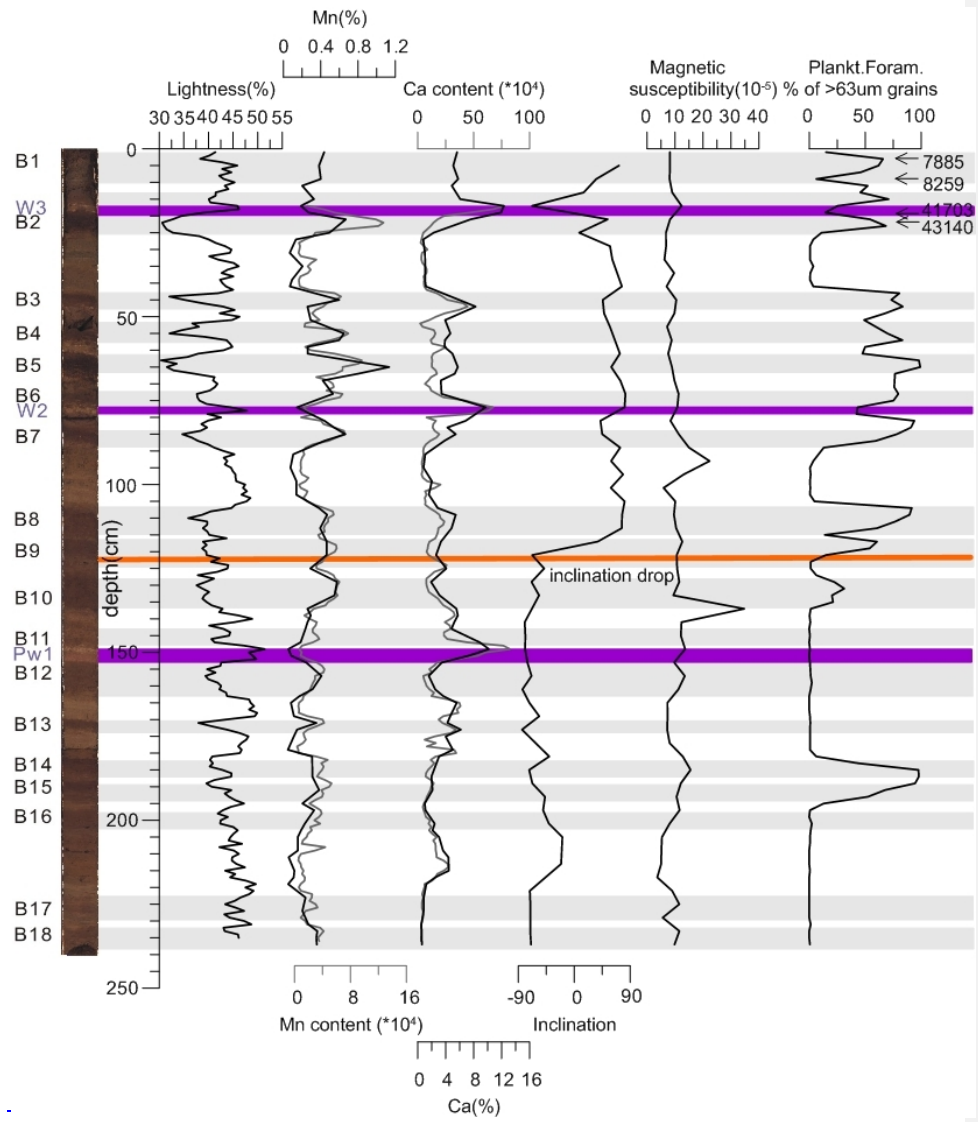
1271

批注 [LP31]: R2: In Figure 1, there is no difference between the Banks and Victoria islands. However, Victoria Island is composed primarily with platformal dolomites, whereas Banks consists mainly of clastic rocks.  
See answer in the response letter.



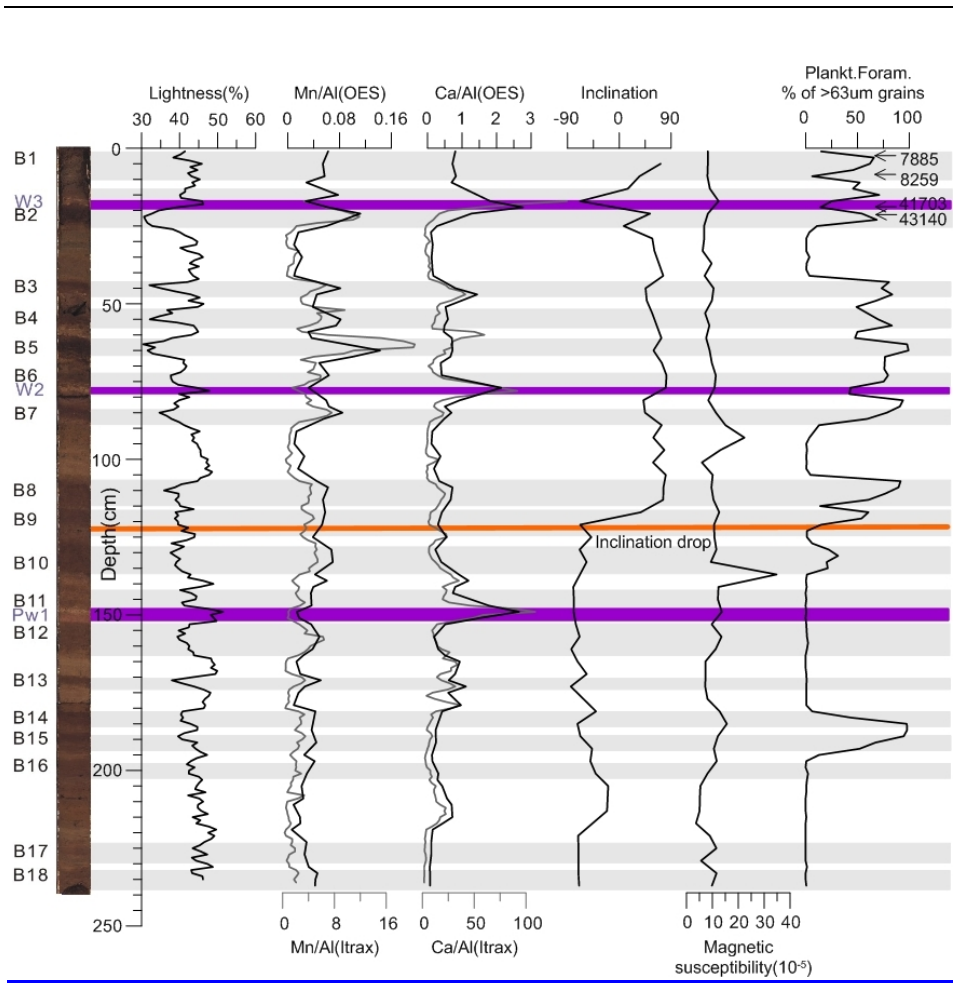
1272  
 1273 **Figure 2.** Index map showing the location of core ARC4-BN05 (yellow circle) and  
 1274 other cores from previous studies mentioned in this paper (red circles). LR, MR, AR,  
 1275 and NR are Lomonosov, Mendeleev, Alpha, and Northwind ridges, respectively; NGS  
 1276 is Norwegian–Greenland Sea. White lines show maximal Pleistocene limits  
 1277 reconstructed for Greenland, Laurentide, Eurasian, and East Siberian Ice Sheets (GIS,  
 1278 LIS, EAIS and ESIS; England et al., 2009; Svendsen et al., 2004; Niessen et al., 2013).  
 1279 Proposed flow lines for grounded ice sheets and ice shelves (red and white arrows,  
 1280 respectively) are after Niessen et al. (2013).  
 1281

1282



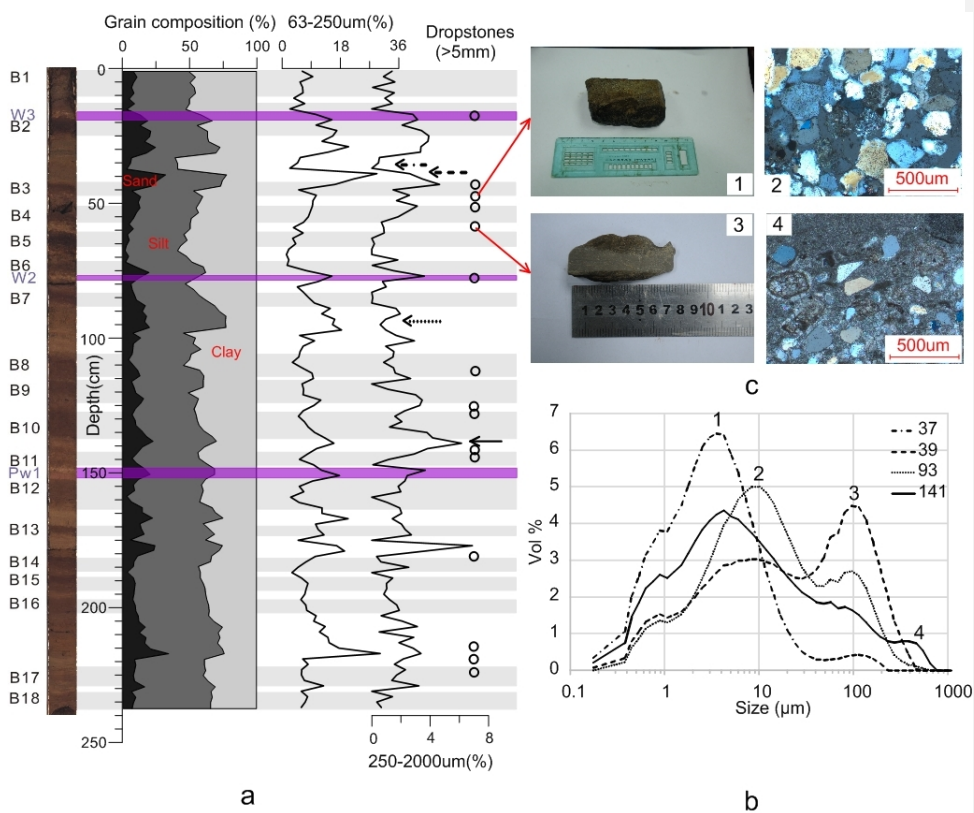
1283

1284 [Old version \(deleted\)](#)



1285

1286 **Figure 3.** Lithostratigraphy and major proxies in core BN05: core photograph with  
 1287 brown layer indices, lightness, Ca and Mn content (bulk XRF –grey line, ICP-OES –  
 1288 black line), paleomagnetic inclination, planktic foraminiferal abundance, and AMS<sup>14</sup>C  
 1289 datings. Predominantly dark brown intervals B1-B18 are highlighted in grey; high-Ca,  
 1290 pink-white layers are marked by purple lines. The main inclination drop is marked by  
 1291 orange line. See Table S1 for data used.



1292

1293 **Figure 4. (a)** Down-core grain-size distribution in core ARC4-BN05 (in volume %):

1294 clay (<4 µm), silt (4-63 µm), sand (63-2000 µm), fine sand (63-250 µm), and coarser

1295 sediment (250-2000µm). Occurrence of dropstones > 5mm is shown by circles on the

1296 right. See Fig. 3 for lithostratigraphy explanation, and Tables S1-2 for data used. (b)

1297 Granulometric distribution types exemplifying major grain-size modes 1-4. Position

1298 of respective curves in core ARC4-BN05 is indicated in the legend (depth in core, cm)

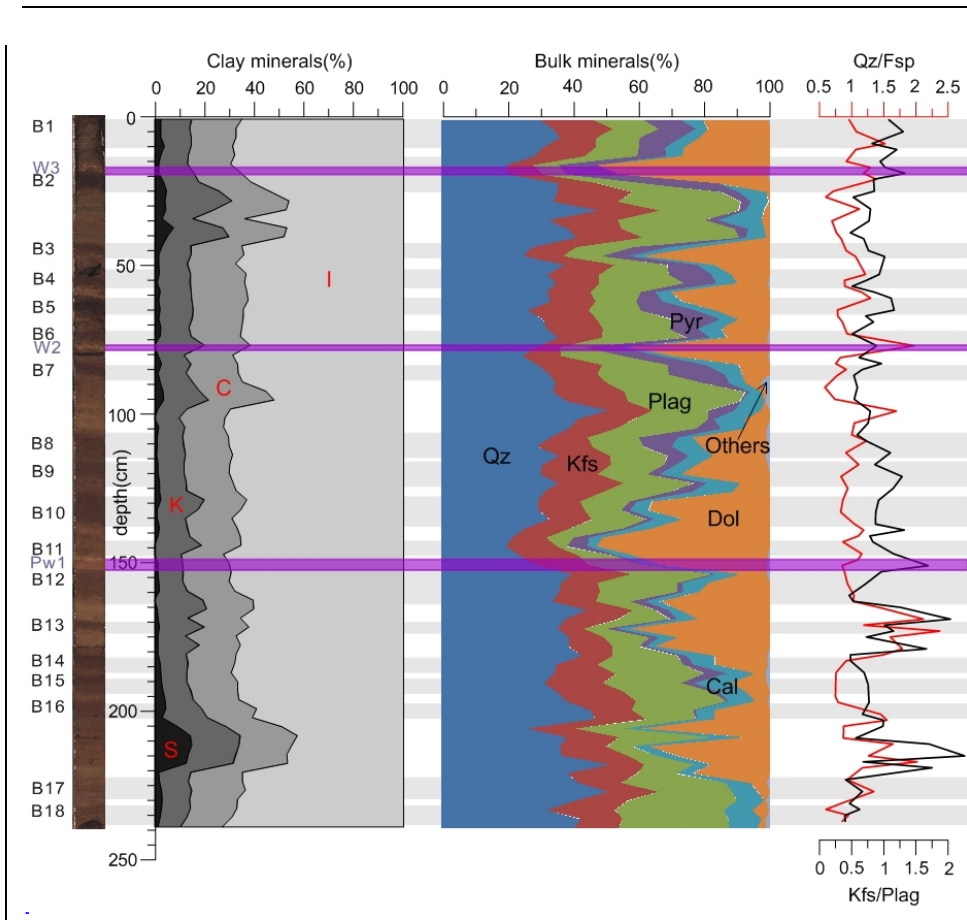
1299 and is shown by arrows in panel a. (c) Examples of dropstones from core ARC4-BN05.

1300 1: 48-54cm, quartz sandstone; 2: same dropstone, thin section in cross polarized light;

1301 3: 56-63.5cm, dolomite dropstone; 4: same dropstone, thin section in cross polarized

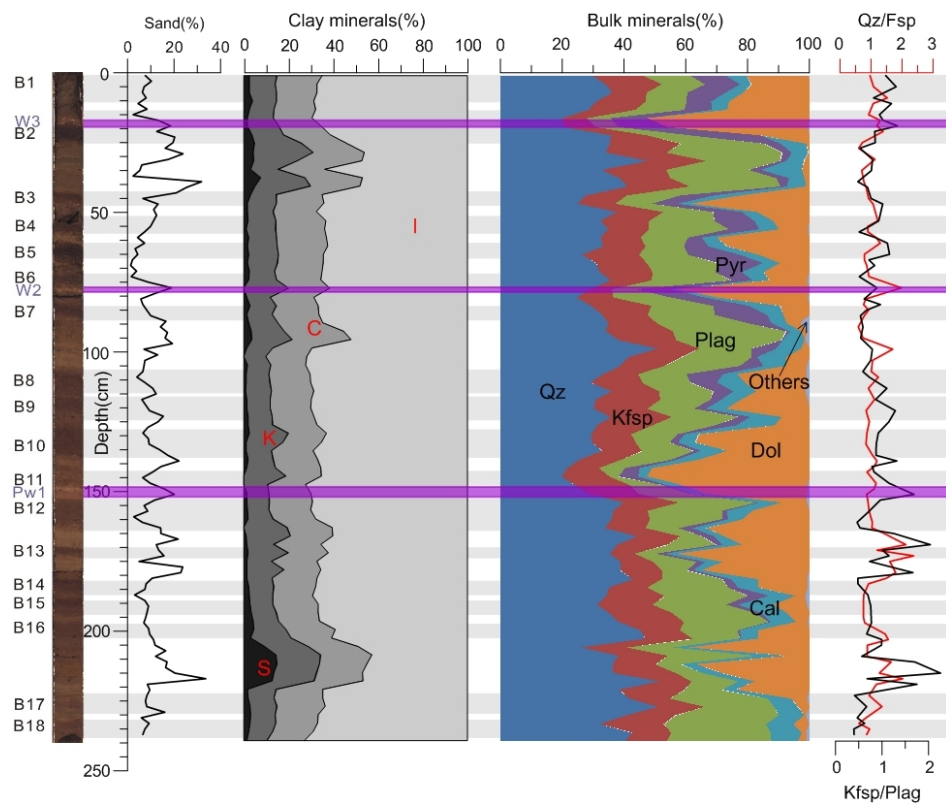
1302 light.

批注 [LP32]: R1 Specify if wt% or vol% are used  
Done



1303  
 1304  
 1305

[Old version \(deleted\)](#)

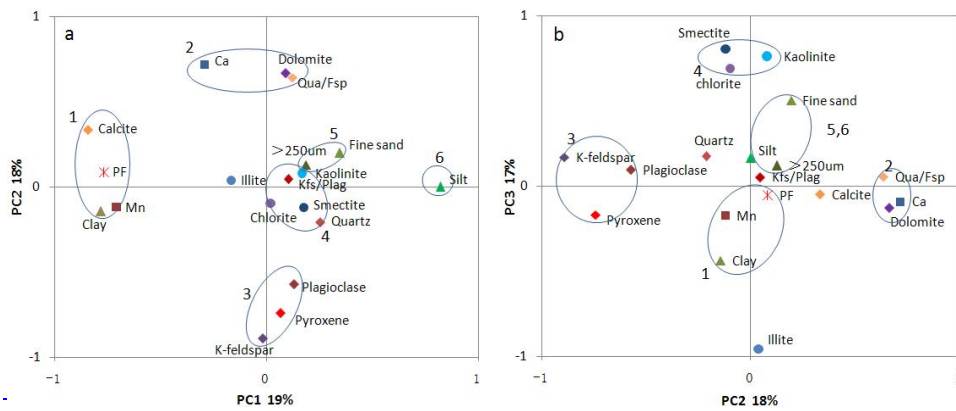


1306

1307 **Figure 5.** Relative weight contents of major clay mineral groups in the clay fraction  
 1308 (<2 μm), bulk mineral composition and related indices in core ARC4-BN05.S, K, C,  
 1309 and I indicate smectite, kaolinite, chlorite, and illite, respectively. Qz, Kfsp, Plag, Pyr,  
 1310 Cal, and Dol are quartz, K-feldspar, plagioclase, pyroxene, calcite, and dolomite,  
 1311 respectively. See Fig. 3 for lithostratigraphy explanation and Table S1 for data used.

1312  
 1313  
 1314  
 1315  
 1316  
 1317  
 1318  
 1319  
 1320  
 1321  
 1322

批注 [LP33]: R2: For the convenience of sedimentary environments analysis, the distribution of the sand fraction should be added to the Figure 5  
 Done



1323

1324 **Deleted**

1325 **Figure 6.** Biplots of Principal Component loading scores in PC 1-2 (a) and PC 2-3 (b)  
 1326 space. Sedimentary variable groups or end-members revealed by the loading  
 1327 distribution are enclosed by ellipses and numbered (see Table 3 and text in section 5.2  
 1328 for discussion). See Tables S3-4 for correlation between variables and PC loading  
 1329 scores.

1330

1331

1332

1333

1334

1335

1336

1337

1338

1339

1340

1341

1342

1343

1344

1345

1346

1347

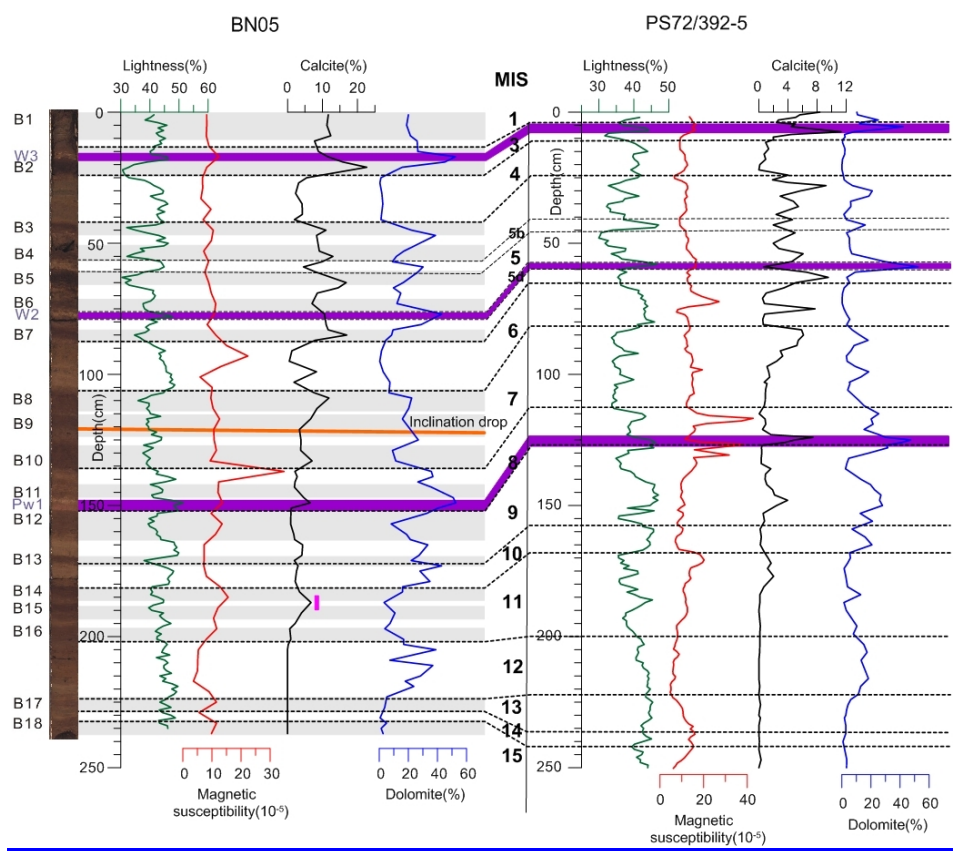
1348

1349

批注 [LP34]: R1: If significant loadings are greater than 0.7 (or smaller than -0.7), then only groups 1,2,3 make sense in Fig. 6a, and groups 3,4,2 - in Fig. 6b. Hence, interpretations in Table 3 should be revised (e.g. group 5 can be eliminated)  
 Plotting and explanation has been revised (see new Fig. 7, Table 3, and explanations in the Discussion)







1355

1356 **Fig.76.** Stratigraphic correlation of core BN05 with PS72/392-5 (Stein et al., 2010a)

1357 based on sediment lightness, magnetic susceptibility, calcite and dolomite content.

1358 See Fig. 3 for [other stratigraphic proxies and lithostratigraphy explanation](#). [Vertical](#)

1359 [magenta bar indicates position of foraminiferal peak in B14-15.](#)

1360

1361

1362

1363

1364

1365

1366

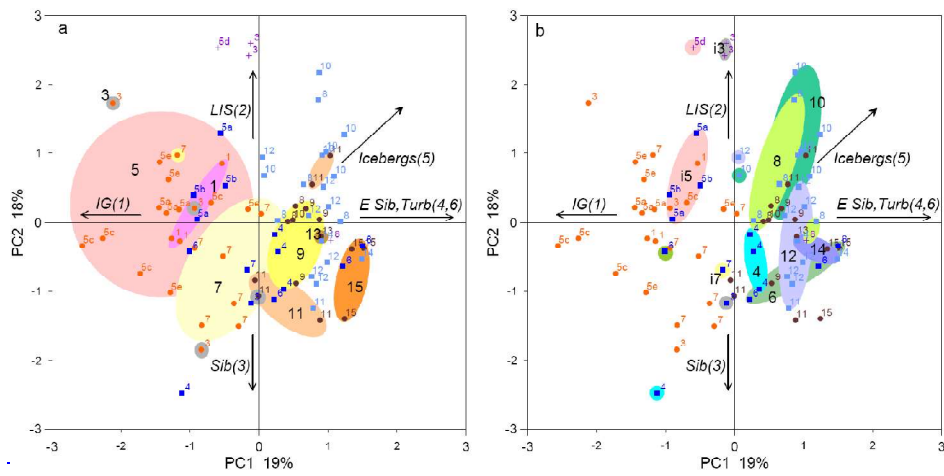
1367

1368

1369

1370

1371



1372

1373 ~~Deleted~~

1374 ~~Figure 8. Biplots of downcore PC scores in the PC 1-2 space grouped by interglacial~~

1375 ~~(a) and glacial intervals (b). Interpretation of loading score distribution: IG —~~

1376 ~~interglacial environments, LIS — Laurentide Ice Sheet provenance, Sib/E Sib —~~

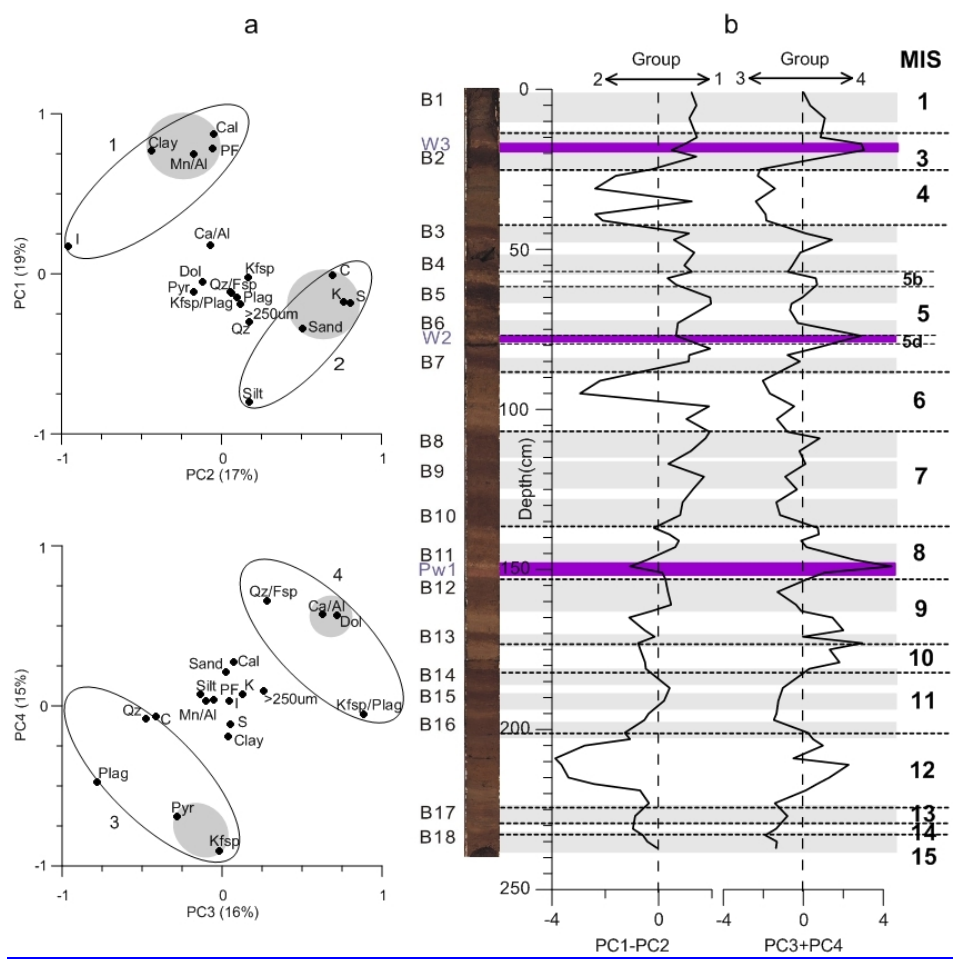
1377 ~~Siberian/East Siberian provenance, Turb. — turbidites; variable group numbers shown~~

1378 ~~in parentheses (Fig. 6; Table 3; see Section 5.2 above for more discussion). Numbers~~

1379 ~~for individual and grouped samples show Marine Isotope Stages. See Table S5 for~~

1380 ~~downcore PC score distribution.~~

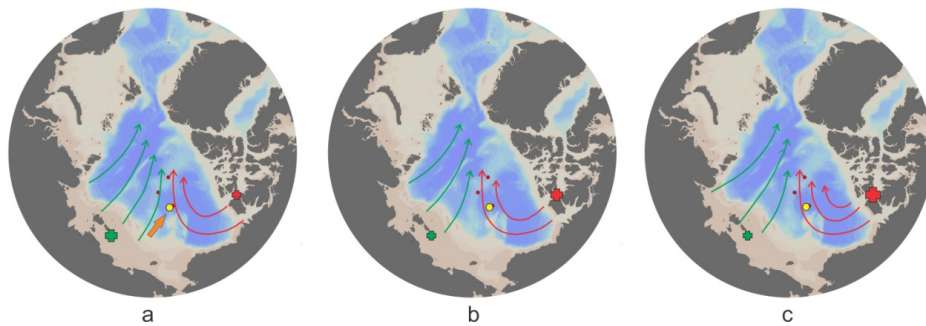
1381



1382  
 1383  
 1384  
 1385  
 1386  
 1387  
 1388  
 1389  
 1390  
 1391  
 1392

**Figure 7. (a)** Biplots of Principal Component loading scores in PC 1-2 and PC 3-4 space (see Table S4 for loading data and Table S3 for correlation between variables). Sedimentary variable groups revealed by the loading distribution are enclosed by ellipses and numbered, with the closest groupings highlighted in grey. **(b)** Downcore distribution of sedimentary variable groups plotted using combined PC 1-2 and PC 3-4 scores (see Table S4 for score data).

批注 [LP35]: R1: Better include Table S4 as a table in the paper  
 Done.



1393

1394

1395

1396

1397

1398

1399

1400

1401

1402

1403

**Figure 98.** Schematic reconstruction of glacial environments in the western Arctic Ocean and factors controlling sedimentation at the BN05 site (yellow circle): surface circulation (red and green arrows), glaciatorbidites (orange filled arrow), and [relative](#) ice-sheet size (red and green crosses). See Fig. 1 for modern circulation. (a) High ESIS inputs: MIS 4, 6, 12, and 14; (b) high LIS inputs: MIS 8 and 10; (c) especially high LIS inputs: intra-MIS5 and 3.